The Search for Higgs Boson Production in Association with a Top-Quark Pair in pp Collisions at $\sqrt{s} = 8$ TeV in the Lepton Plus Jets Final State

John Garland Wood

Charlottesville, VA

B.S., The University of California, Berkeley, 2008

A Dissertation presented to the Graduate Faculty

of the Unversity of Virginia in Candidacy for the Degree of

Doctor of Philosophy

Department of Physics

University of Virginia

May, 2015

Abstract

The most important goal of the Large Hadron Collider (LHC) is to elucidate the mechanism of electroweak symmetry breaking. The Standard Model (SM) Higgs boson is thought to be a prime candidate for this. The newly discovered boson announced on July 4th, 2012, with a mass of ∼125 GeV/c^2, has so far been shown to be consistent with a SM Higgs. However, the final confirmation of this new particle as the SM Higgs depends on subsequent measurements of all of its properties. The observation of this new particle in association with top-quark pairs would allow the couplings of this particle to top and bottom quarks to be directly measured. $t\bar{t}H$, with Higgs decaying to $b\bar{b}$ is an excellent channel to explore due to the dominant branching ratio of Higgs to $b\bar{b}$ and the kinematic handle the $t\bar{t}$ system offers on the event. However, it presents a plethora of difficult challenges due to a low signal to background ratio and uncertainties on kinematically similar SM backgrounds. This work discusses the search for Higgs boson production in association with a top-quark pair in pp collisions at $\sqrt{s} = 8$ TeV, collected by the Compact Muon Solenoid (CMS) experiment at the LHC. The search has been performed and published in two stages. The first analysis used the first 5.1 fb^{-1}, and was followed up by the second analysis with the full 2012 dataset, using a total integrated luminosity of 19.5 fb^{-1}

We approve the dissertation of John Garland Wood.

Date of Signature

Supervisor: Dr. Christopher Neu

Committee Chair: Dr. Bradley Cox

Committee Member: Dr. Hank Thacker

PhD Committee Chair: Dr. Astronomy Person

Contents

List of Figures

List of Tables

Chapter 1

Introduction

On July 4th, 2012, the Compact Muon Solenoid (CMS) and A Toroidal LHC Apparatus (ATLAS) experiments announced the discovery of a new boson of mass $\sim$ 125 GeV/c^2 [1] [2]. The particle has been shown to be increasingly consistent with the description of the boson predicted by the Higgs mechanism of the SM, as measurements on its mass, width, and quantum numbers are completed. However, there are several properties of this new boson, which remain to be tested. Figure 1.1 shows a consistent mass peak betwen the $H \to ZZ$ and $H \to \gamma\gamma$ channels at the CMS experiment.

The Yukawaka coupling of the Higgs boson to the top-quark in the SM is the largest coupling among the fundamental particles and is well predicted - thus offering an excellent test of the nature of the coupling of the Higgs to fermions, as well as a potential probe into pysics Beyond the Standard Model (BSM) that would alter this value from the SM prediction. The production of the Higgs boson in association with top-quark pairs is the best production mode at the LHC that offers direct access to the top-Higgs coupling. The dominant production mode of Higgs at the LHC, gluon-gluon fusion, involves a triangle loop of strongly-coupled fermions, which

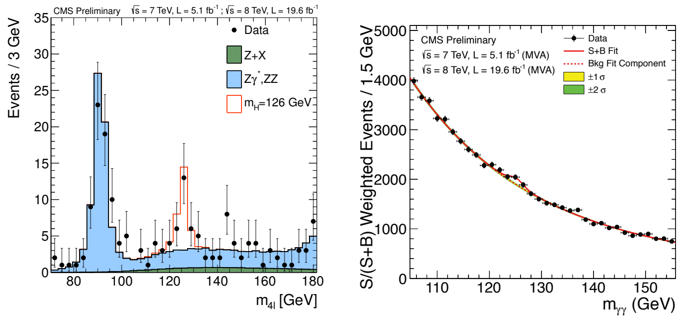

(a) CMS results for the $H \to ZZ$ channel

(b) CMS results for the $H \to \gamma\gamma$ channel

Figure 1.1: The CMS experiment has observed a new boson at m$\sim$125 GeV/c^2

includes all of the other quarks, as well as the potential for BSM particles.

$t\bar{t}H$ production also has the ability to constrain some extensions of the SM that would not modify the Higgs branching fractions enough to be seen within current experiemental precision. Such models include Little Higgs models, models with extra dimensions, top-color models, and composite Higgs models that introduce a vector-like top partner, a t', that can decay to tH, bW, or tZ states. Both $t't'$ and $t't$ production would produce a $t\bar{t}H$ final state, or one that is indistinguishable from it ($tHbW$). Upper limits on $t\bar{t}H$ production would also provide limits on the previously described models, which would be complementary to existing direct searches for t' particles, which attempt to reconstruct the t' resonance.

The $t\bar{t}H$ channel has a rich set of possible final states. Each top-quark will decay to a b-quark and a W boson. The W boson will subsequently decay to two quarks, or a lepton and a neutrino. These decays are classified as either hadronic, semi-leptonic, or di-leptonic for zero, one, or both t quarks decaying leptonically respectively. The Higgs may to decay to b-quark, W, Z, τ, or γ pairs. In fact, this is one of the only production modes at the LHC which has access to every Higgs decay mode, as other production mechanisms are swamped by large backgrounds preventing measurements of all Higgs decay types.

The search is performed with the CMS experiment, a modern, general purpose particle detector capable of reconstructing and identifying hadronic jets, photons, electrons, muons, and tau leptons. The hermetic design, and it's high precision and efficiency in reconstrucing and tracking every particle in a pp collision, also makes it suitable for reconstructing missing transverse energy from the calculated momentum imbalance of all of the measured particles in the event. This missing transverse energy is often the signature of a neutrino, which is the only SM particle capable of escaping detection. The detector uses a 3.8 T axial magnetic field, produced by the solenoid it is named after, to bend charged particles as they travel through the detector. The measured curvature of their tracks allows the momentum of the particles to be calculated with to a high precision. Tracks are formed and particles are reconstructed by a combination of sub-detector systems which work together to form the final final reconstructed image of each particle in the collision.

This thesis will focus on a semi-leptonic decay of the top-quarks, with the Higgs decaying to a b-quark pair. Figure 1.2 is Feynman diagrm of the $t\bar{t}H$ process. The largest background to this process is top-quark pair production with extra jets originating from Initial State Radiation (ISR) or Final State Radiation (FSR) radiation, $t\bar{t}+jets$. The irreducible background is formed by top-quark pairs, where a gluon is radiated and decays to b-quark pairs, $t\bar{t}+b\bar{b}$. In addition to the large backgrounds, the high jet multiplicity in the $t\bar{t}H$ final state gives rise to a combinatorics problem in associating each jet with its role in the $t\bar{t}H$ system. This inevitably leads to

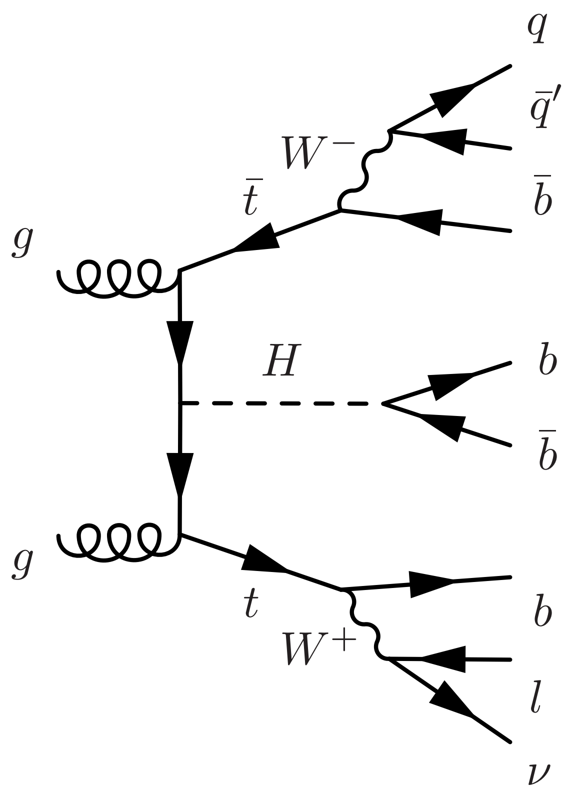

Figure 1.2: A Feynman diagram of the $t\bar{t}H$ process, with Higgs$\rightarrow b\bar{b}$, and the $t\bar{t}$-system decaying semi-leptonically

misidentifying which jets are the decay product of the Higgs, and thus additionally smears out the resolution on the mass of the Higgs. Due to the similarity of the $t\bar{t}+b\bar{b}$ background and the combinatorics issue, no single variable is suitable for signal extraction. A Multi-Variate Analysis (MVA) technique is used in an attempt to isolate the $t\bar{t}H$ signal from the $t\bar{t}+jets$background. The MVA provides a one-dimensional discriminant based on several input variables related to the kinematics of the event. This discrimant is then used to perform signal extraction and set upper-limits on $t\bar{t}H$ production. The results of two searches will be presented. The first result used the first 5.1 fb^{-1} of the 2012 dataset, with center of mass energy of 8 TeV, and was published in the Journal of High Energy Physics (JHEP), May 2013. The second result was update with the full 19.4 fb^{-1} 8 TeV dataset, and was published in JHEP, Spetember 2014.

Chapter 2

Theoretical Background

The Standard Model (SM) of particle physics represents the sum of knowledge of the fundamental particles and their interactions with each other. It is a Quantum Field Theory (QFT) that represents the interactions of each of the fundamental forces through the symmetry of a mathematical object known as a Lie group. It is the theory that dictates the rate that the $t\bar{t}H$ process is produced, as well as the kinematics of every particle involved. As such, its predictions are critical for modeling the charateristic signature of the $t\bar{t}H$ signal in the CMS detector, as well as the background processes, like $t\bar{t} + b\bar{b}$ which leave a kinematically similar final state signature.

2.1 An Overview of Quantum Field Theory

Quantum Field Theory (QFT) was developed out of the need for a relativistic description of quantum mechanics. Since the Einstein relation $E = mc^2$ allows for the creation of particle-antiparticle pairs, the single-particle description used in non-relativistic quantum mechanics, fails describe this phenomenom [3]. This additionally fails when considering that Heisenberg's uncertainty relation, $\Delta\ E \cdot\ \Delta\ t = \hbar$, allows for an arbitrary number of intermediate, virtual particles to be created. By quantizing a field representing a certain type of particle, multiparticle states are naturally described as discreet excitations of that field.

Lorentz invariance, and the need to preserve causality, also define a fundamental relationship between matter and antimatter. The propagation of a particle across a space-like interval is treated equivalently to the an anti-particle propagating in the opposite direction [3]. This is done so that the net probability amplitude for the particles to have an effect on a measurment occuring accross a space-like interval cancel each other, thus preserving cuasality. This cancellation requirement additionally implies that the particle and anti-particle have the same mass, with opposite quantum numbers such as spin or electric charge.

The Lorentz transformations for a scalar field are different than for a field with internal degrees of freedom, such as spin. A rotation on a vector field, will affect both its location, as well as it's orentation [3]. This means the Lorentz invariant equation of motion descirbing a scalar field will have a different form than equations of motion for a field with spin. The most relevant equations describe the particles of SM, which contain spins of 0, 1/2, and 1. They are described by the Klein-Gordan, Dirac, and Proca equations respectively.

Klein-Gordon equation, for scalar (spin 0) fields

$$(\partial^2 + m^2)\phi = 0 \tag{2.1}$$

Dirac equation, for spinor (spin 1/2) fields

$$(i\gamma^\mu \partial_\mu - m)\psi = 0 \tag{2.2}$$

Proca equation, for vector (spin 1) fields

$$\partial_\mu(\partial^\mu A^\nu - \partial^\nu A^\mu) + m^2 A^\nu = 0 \tag{2.3}$$

With these equations, one can build a theory of free particles. The Lagrangian formulation is the most appropriate since all expressions are explicitly Lorentz invariant [3]. The Lagrangians for the Klein-Gordon, Dirac, and Proca equations are given as:

Klein-Gordon Lagrangian, for real and complex scalar fields

$$\begin{aligned} \mathcal{L} &= \partial_\mu \partial^\mu \phi^2 - \frac{1}{2} m^2 \phi^2 \\ \mathcal{L} &= (\partial_\mu \phi)^* (\partial^\mu \phi) - m^2 (\phi)^* (\phi) \end{aligned} \tag{2.4}$$

Dirac Lagrangian, for spinor fields

$$\mathcal{L} = i\bar{\psi}\gamma^\mu \partial_\mu \psi - m\bar{\psi}\psi \tag{2.5}$$

Proca Lagrangian, for vector fields

$$\mathcal{L} = -\frac{1}{4} F_{\mu\nu} F^{\mu\nu} + m^2 A^\nu A_\mu \tag{2.6}$$

where $F_{\mu\nu}$, is the field strength tensor, defined as $F_{\mu\nu} = \partial_\mu A_\nu - \partial\nu A_\mu$

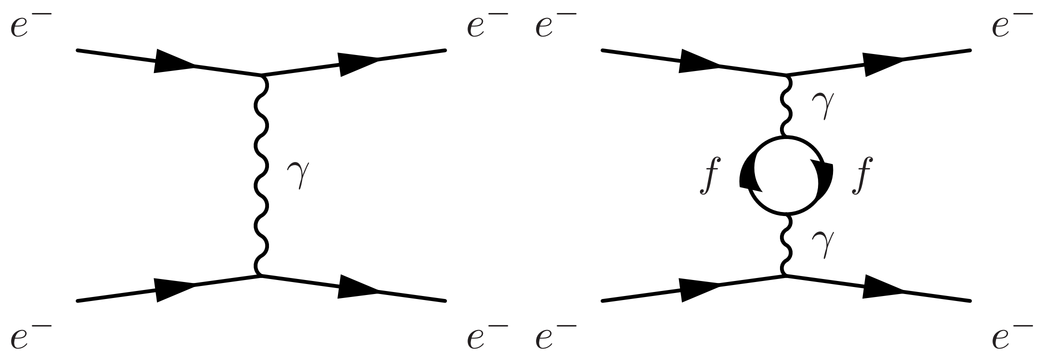

(a) A LO Feynman diagram (b) A NLO Feynman diagram

Figure 2.1: Leading and Next to Leading Order Feynman diagrams for the coulomb scattering process

Interactions are generated by coupling multiple fields together in a single term, such as $ieA_\mu\bar{\psi}\psi$ and treating it as a perturbation to the free field theory. This implies every interaction between particles is carried out by a virtual mediating particle. When two electrons scatter off one another, they are really exchanging a virtual photon, the mediator of the electromagnetic force. The $W^{\pm} andZ$ bosons mediate the weak force, while the $gluons$ mediate the strong force.

$$\mathcal{L} = \mathcal{L}_{Free} + \mathcal{L}_{Interacting} \tag{2.7}$$

In order to calculate the probability and dynamics of two particles interacting with one another, an integral, constrained by energy and momentum conservation, over the phase space of outgoing particles and the scattering amplitude, $mathcalM$, is evaluated. The scattering amplitude is calculated by using the propagtor (Green's function of the free particle theory) for the incoming, mediating, and outgoing particles, with an appropriate wieghting function, or vertex factor, for each point the particles interact in the scattering process, and then integrating over the momentum of the mediating particle. Richard Feynmann developed a set of rules for the writing down the propagators and vertex factors directly from the Lagrangian, and easily computing the scattering amplitude. He also introduced an elegant pictographic notation useful for visualizing particle interactions, known as Feynmann diagrams.

With these tools, one can calculate the probability amplitudes of a given process occuring to Leading Order (LO) without any difficulties. However, when calculations in Next to Leading Order (NLO) are performed, and loop diagrams of virtual particles are considered, the probability amplitudes associated with a given process diverge to infinity. This occurs when one integrates over all of the possible momentum allowed by intermediate, loops of virtual particles, which due to Heisenberg's uncertainty principle, are allowed to take on any value of momentum. Figure 2.1 shows an example of a LO and NLO process.

The systematic removal of divergences from a theory is called renormalization. The di-

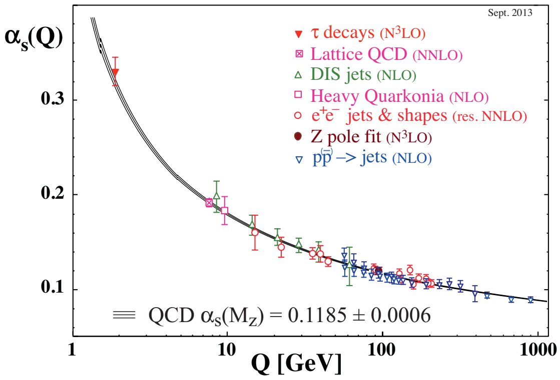

Figure 2.2: The global average of α_s, the QCD coupling constant.

vergences are absorbed into the definitions of the free parameters of the theory, making the parameters a function of the energy scale the process occurs at, instead of a constant. This allows for the calculations of fundamental processes to completed, as long as the energy scale of the interaction is known. A modern interpretation of renormalization was provided by Kenneth Wilson [4] [5]. Instead of seeing the effects of high momentum calculations after moving to NLO in perturbation theory, one uses an effective Lagrangian, computed by integrating out shells of momentum beginning at the energy cutoff of the theory, where the NLO effects begin the dominate. The dimensions of integration are then rescaled and the result of evaluating the integral over the momentum shell is absorbed into the definition of free parameters. The processes is iterated until the energy scale of the interaction is reached. The functional dependence of the parameters is then directly present in the resulting effective Lagrangian, instead of appearing suddenly when accounting for the one-loop contributions at NLO. Regardless of how strange this procedure seem, the running of the coupling constant as a function of interaction engergy has been validated experimentally time and time and again, as shown in Figure 2.2 [6].

2.2 Abelian Gauge Theories of Particle Interactions

In 1930, Herman Weyl introduced the idea that the interactions between fields can be generated by requiring them to be invariant under guage tansformations of a local symmetry [7]. For electromagnetism, the local symmetry is that of the Lie group, $U(1)$. It is an abelian group, which has the property that the generators of the group symmetry commutes with themselves. The $U(1)$ symmetry is invariant under phase rotations. By requiring local guage invariance, the Lagrangian must be unchanged under the

$$\psi(x) \rightarrow e^{i\alpha(x)}\psi(x). \tag{2.8}$$

Consider the Lagrangian for a free spin 1/2 particle:

$$\mathcal{L} = \bar{\psi}(i\gamma^\mu \partial_\mu - m)\psi \tag{2.9}$$

The first term in the Lagrangian, involving the derivative, acts on $\alpha(x)$, creating a new term in the Lagrangian, breaking its invariance under the local phase transformation.

$$\mathcal{L} \to \mathcal{L} - (\partial_\mu \alpha)\bar{\psi}\gamma^\mu \psi \tag{2.10}$$

Thus, a new term must be added to the orginial Lagrangian to cancel out the term arising from the local phase transformation. This is achieved by defining the covariant derivative:

$$D_\mu = \partial_\mu + ieA_\mu \tag{2.11}$$

where A_μ is a new vector field that transforms as follows:

$$A_\mu(x) \to A_\mu(x) - \frac{1}{e}\partial_\mu \alpha(x) \tag{2.12}$$

The covariant derivative thus transforms like

$$\begin{aligned} D_\mu \psi(x) &\to [\partial_\mu + ie(A_\mu - \frac{1}{e}\partial_\mu \alpha)]e^{i\alpha(x)} D_\mu \psi(x) \\ &= e^{i\alpha(x)}[\partial_\mu + ie(A_\mu - \frac{1}{e}\partial_\mu \alpha + \frac{1}{e}\partial_\mu \alpha)] D_\mu \psi(x) \\ &= e^{i\alpha(x)}(\partial_\mu + ieA_\mu)\psi(x) \\ &= e^{i\alpha(x)} D_\mu \psi(x) \end{aligned} \tag{2.13}$$

This covariant derivative transforms in the smae way that $\psi(x)$ does, and the new locally guage invariant Lagrangian becomes

$$\begin{aligned} \mathcal{L} &= \bar{\psi}(i\gamma^\mu D_\mu - m)\psi - \frac{1}{4}F^{\mu\nu}F_{\mu\nu} \\ &= i\bar{\psi}\gamma\partial_\mu \psi - \bar{\psi}\gamma^\mu \psi\ A_{mu} - m\bar{\psi}\psi - \frac{1}{4}F^{\mu\nu}F_{\mu\nu} \end{aligned} \tag{2.14}$$

where

$$F^{\mu\nu} = (\partial^\mu A^\nu - \partial^\nu A^\mu) \tag{2.15}$$

and $\frac{1}{4}F^{\mu\nu}F_{\mu\nu}$ is the kinetic energy term of the Proca equation for the new vector field.

This new Lagrangian is identical to the QED Lagrangian, excpet it was derived beginning with a free dirac theory and requiring the field to be locally guage invariant under $U(1)$ transformations. This necessitated the introduction of a new vector field, A_μ, as well as an interaction term with it. This implies that the electromagnetic force can be represented by the requirement of local $U(1)$ symmetry on a free Dirac particle.

It should be noted, that if the photon had mass, an additional term from the Proca equation would have to be added to the Lagrangian, $m^2 A_\mu A^\mu$. This term complicates the picture since it is not invariant under local phase transformations, and cannot be compensated for through a different choice of A_μ. This implies that the bosons of a guage theory must be massless in order to preserve local guage invariance.

2.3 Non-Abelian Gauge Theories of Particle Interactions

In 1954, Yang and Mills worked to extend this idea to symmetries of different guage groups [8]. Their most imortant accomplishment was developing this procedure for non-abelian groups. These are groups, where the transformation does not involve a simple variable $\alpha(x)$, but rather an entire matrix of dimension n>2. These matrices do no commute with each other, and their work developed the procedure for applying local guage invariance described above to the more complex, higher dimensional symmetries, such as $SU(2)$ and $SU(3)$. Consider the case of $SU(2)$ symmetry. The theory is appropriate for describing the dynamics of two fermion fields, represented as a doublet:

$$\psi = \begin{pmatrix} \psi_1(x) \\ \psi_2(x) \end{pmatrix} \tag{2.16}$$

this will transform under the $SU(2)$ transformation as a two-component spinor:

$$\psi \rightarrow \ \exp\langle \ i\alpha^i \frac{\sigma_i}{2} \rangle \psi \tag{2.17}$$

where σ^i are the Pauli matrices:

$$\sigma^1 = \begin{pmatrix} 0 & 1 \\ 1 & 0 \end{pmatrix} \ , \sigma^2 = \begin{pmatrix} 0 & -i \\ i & 0 \end{pmatrix} \ , \sigma^3 = \begin{pmatrix} 1 & 0 \\ 0 & -1 \end{pmatrix} \tag{2.18}$$

and have the commutation relation defined by:

$$[\frac{\sigma^i}{2}, \frac{\sigma^j}{2}] = i\epsilon^{ijk} \frac{\sigma^k}{2} \tag{2.19}$$

Similar to the case of the $U(1)$ Abelian symmetry, in order to form a lagrangian that is locally guage invariant, three vector fields, A^i_μ, $i = 1, 2, 3$, are introduced, and coupled to ψ through the covariant derivative:

$$D_\mu = (\partial_\mu - igA^i_\mu \frac{\sigma^i}{2}) \tag{2.20}$$

to ensure that the derivative covaries with the transformation, the fields, A^i_μ will transform like:

$$A^i_\mu \frac{\sigma^i}{2} \to A^i_\mu \frac{\sigma^i}{2} + \frac{1}{g}(\partial_\mu \alpha^i)\frac{\sigma^i}{2} + i[\frac{\alpha^i \sigma i}{2}, A^i_\mu \frac{\sigma^i}{2}] \tag{2.21}$$

The third term, which was absent from the abelian form of the transformation, is necessary to account for the non-commutation of the pauli matrices. This non-communtation also changes the form of the field strength tensor, $F^i_{\mu\nu}$:

$$F^i_{\mu\nu} = \partial_\mu A^i_\nu - \partial_\nu A^i_\mu + g\epsilon^{ijk} A^j_\mu A^k_\nu \tag{2.22}$$

The entire $SU(2)$ invariant Lagrangian can then be written as:

$$\begin{aligned} \mathcal{L}_{Yang-Mills} &= -\frac{1}{4} F^i_{\mu\nu} F^{i\mu\nu} + \bar{\psi}(i\gamma^\mu D_\mu)\psi \\ &= -\frac{1}{4} F^i_{\mu\nu} F^{i\mu\nu} + \bar{\psi}(i\gamma^\mu \partial_\mu - igA^i_\mu \frac{\sigma^i}{2})\psi \end{aligned} \tag{2.23}$$

This procedure generalizes to any continuous group of symmetries. The basic steps involve identrifying the generators of the transformation:

$$\psi(x) \to e^{i\alpha^a t^a} \psi \tag{2.24}$$

where t^a are a set of matrices with the commutation relationship:

$$[t^a, t^b] = if^{abc} t^c \tag{2.25}$$

where f^{abc} is the structure constant for the goup. The covariant derivative is then defined as:

$$D_\mu = \partial_\mu - igA^a_\mu t^a \tag{2.26}$$

where the fields, A^a_μ, transform like:

$$A^a_\mu \to A^a_\mu + \frac{1}{g}\partial_\mu \alpha^a + f^{abc} A^b_\mu \alpha^c \tag{2.27}$$

the field strength tensor is then formed as:

$$F^a_{\mu\nu} = \partial_\mu A^a_\nu - \partial_\nu A^a_\mu + f^{abc} A^b_\mu A^c_\nu \tag{2.28}$$

and finally, the locally, gauge invariant Lagrangian will have the form:

$$\begin{aligned}\mathcal{L}_{\text{General, non-Abelian}} &= -\frac{1}{4}F^a_{\mu\nu}F^{a\mu\nu} + \bar{\psi}(i\gamma^\mu D_\mu)\psi \\ &= -\frac{1}{4}F^a_{\mu\nu}F^{a\mu\nu} + \bar{\psi}(i\gamma^\mu\partial_\mu - igA^a_\mu t^a)\psi\end{aligned} \tag{2.29}$$

In 1964, Murray Gell-Mann and Zweig independtly developed a model of hadron interactions, that described the spectrum of baryons and mesons in terms of combinations of fundamental particles, which Gell-Mann named quarks [9] [10] [11]. In their model, three quarks: u, d, s formed an $SU(3)$ flavor symmetry. However, this did not explain the appearance of only two and three quark combinations, the mesons and baryons. It also could not explain the spin statistics of the baryons. The Δ^{++}, Δ^-, and Ω^-, particles all have uuu, ddd, sss quark combinations, respectively, with their spins aligned. That is to say, these baryons seem to violate the Pauli-exclusion prinicple since all three quarks seem to occupy the same quantum state simultaneously.

In 1964, O.W. Greenberg solved this problem by proposing that quarks also have an additional quantum number, *color*, that come in three types: red, green, blue [12]. The requirement that all stable hadrons be color neutral: either possessing equal amounts of all three colors in qqq combinations, or a $q\bar{q}$ pair sharing the same color, also explained the observation of only 2 and 3 quark combinations in experiments. These three colors form an $SU(3)$ symmetry, and is the gauge symmetry describing the interactions of quarks and leptons. This theory is known as Quantum Chromodynamics (QCD). Its derivation follows from the procedure outlined above. This group has eight generators, kown as the Gell-Mann matrices, and are defined as:

$$\begin{aligned}
&t^1 = \frac{1}{2}\begin{pmatrix}0&1&0\\1&0&0\\0&0&0\end{pmatrix}, t^2 = \frac{1}{2}\begin{pmatrix}0&-i&0\\i&0&0\\0&0&0\end{pmatrix}, t^3 = \frac{1}{2}\begin{pmatrix}1&0&0\\0&-1&0\\0&0&0\end{pmatrix}\\
&t^4 = \frac{1}{2}\begin{pmatrix}0&0&1\\0&0&0\\1&0&0\end{pmatrix}, t^5 = \frac{1}{2}\begin{pmatrix}0&0&-i\\0&0&0\\i&0&0\end{pmatrix}\\
&, t^6 = \frac{1}{2}\begin{pmatrix}0&0&0\\0&0&1\\0&1&0\end{pmatrix}, t^7 = \frac{1}{2}\begin{pmatrix}0&0&0\\0&0&-i\\0&-i&0\end{pmatrix}, t^8 = \frac{1}{2\sqrt{3}}\begin{pmatrix}1&0&0\\0&1&0\\0&0&-2\end{pmatrix}
\end{aligned} \tag{2.30}$$

and a Lagrangian defined as:

$$\begin{aligned}\mathcal{L}_{QCD} &= -\frac{1}{4}G^a_{\mu\nu}G^{a\mu\nu} + \bar{\psi}(i\gamma^\mu D_\mu) \\ &= -\frac{1}{4}G^a_{\mu\nu}G^{a\mu\nu} + \bar{\psi}(i\gamma^\mu\partial_\mu - igA^a_\mu t^a)\end{aligned} \tag{2.31}$$

where t^a are the Gell-Mann matrices defined in equation 2.30 and the fields A^a_μ are the eight mediators of the QCD force, the *gluons*.

Like all non-abelian guage theories, it is asymptotically free. Thus, the strength of the coupling constant, α_s, decreases as the momentum-transfer, Q in interaction increases. This allows the use of perturbation theory for high-momentum calculations, therefore allowing calculations of hadronic-processes for experimental evaluation.

The idea of local guage invariance was successful in describing the dynamics of QED and QCD, which only contain massless guage bosons. Theorists had long postulated that the weak force was so weak because it was being facilitated by massive bosons, but adding a mass term for a boson breaks the local guage invariance. So, a tool was needed to reconcile the concept of local guage invariance, which works so well for the other forces, with the prospect of the weak force being facilitated by massive guage bosons.

2.4 The Higgs Mechanism in an Abelian Theory

In 1964 Peter Higgs introduced the idea that the guage bosons can acquire their mass through the breaking of an underlying symemtry [13]. In other words, the natural symmetry of the Lagrangian describing a particular interaction could be different than the symmetry we observe in nature. Consider an abelian example of complex scalar field theory, coupled to itself and to an electromagnetic field [3].

$$\mathcal{L} = -\frac{1}{4}(F_{\mu\nu})^2 + |D_\mu\phi|^2 - V(\phi) \tag{2.32}$$

where $D_\mu = \partial_\mu + ieA_\mu$, is the familiar coviarant derivative, and the Lagrangian is invariant under the $U(1)$ transformation as described earlier. The potential term, $V(\phi)$ has the form

$$V(\phi) = -\mu^2\phi^*\phi + \frac{\lambda}{2}(\phi^*\phi)^2 \tag{2.33}$$

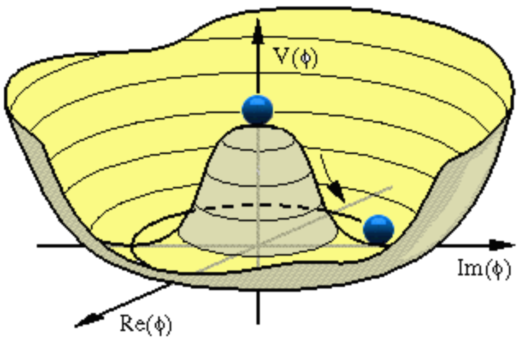

Figure 2.3: A visual representation of the Higgs potential

if $\mu^2 > 0$ the shape of the potential no longer has a mimium at $\langle\phi\rangle = 0$. Figure 2.3 shows a plot of the potential energy of ϕ in terms of each of its components. The new minimum potential energy occurs at:

$$\langle\phi\rangle = \phi_0 = \left(\frac{\mu^2}{\lambda}\right)^{1/2} \tag{2.34}$$

and while the field has a ground state at the zero potential point it is in an unstable equilibrium. Any quantum fluctuation about this point will take the field into the lower energy configuration with a ground state about the new minimum. When the Langrangian is expanded about 2.34, the field, ϕ is rewritten as:

$$\phi(x) = \phi_0 + \frac{1}{\sqrt{2}}(\phi_1(x) + i\phi_2(x) \tag{2.35}$$

the potential term, $V(x)$, then becomes:

$$V(x) = -\frac{1}{2\lambda}\mu^4 + \frac{1}{2}\cdot 2\mu^2\phi_1^2 + \mathcal{O}(\phi_i^3) \tag{2.36}$$

where we can notice that ϕ_1 has acquired a mass term with, $m = \sqrt{2}\mu$, while the scalar field ϕ_2 remains massless, and is known as the Goldstone boson. The covariant derivative is also tranformed as:

$$|D_\mu\phi|^2 = \frac{1}{2}(\partial_\mu\phi_1)^2 + \frac{1}{2}(\partial_\mu\phi_2)^2 + \sqrt{2}e\phi_0\cdot\ A_\mu\partial^\mu\phi_2 + e^2\phi_0^2A_\mu A^\mu + ... \tag{2.37}$$

where cubic and quartic terms of A_μ, ϕ_1, and ϕ_2 have been dropped. The important term is the last one, which can be interpreted as a mass term of the vector field, A_μ

$$\Delta\mathcal{L}_M = \frac{1}{2}m_A A_\mu A^\mu = e^2\phi_0^2A_\mu A^\mu \tag{2.38}$$

where $m_A = 2e^2\phi_0^2$, has arisen from consequences of a non-zero vacuum expectation value of the ϕ field. The remaining, massless Godlstone boson, ϕ_2 is not a physical particle, but rather a consequence of the choice of guage. This is illustrated when we can use the $U(1)$ guage symmetry to rotate the field $\phi(x)$ such that the field disapears.

$$\begin{aligned}\phi \to \phi' &= e^{i\alpha}(\phi_1 + \phi_2)\\ &= (\cos\alpha + i\sin\alpha)(\phi_1 + \phi_2)\\ &= (\phi_1\cos\alpha - \phi_2\sin\alpha) + i(\phi_1\sin\alpha + \phi_2\cos\alpha)\\ &= (\phi_1 - \phi_2\tan\alpha) + i(\phi_1\tan\alpha + \phi_2)\end{aligned} \tag{2.39}$$

Choosing $\alpha = -\tan\phi_2/\phi_1$ will make ϕ' a real quantity and elminate it's imaginary component, ϕ_2'. The lagrangian can then be rewritten in terms of the rotated field ϕ' and see that massless boson is indeed removed from the theory.

$$\begin{aligned}\mathcal{L} = &\frac{1}{2}(\partial_\mu \phi_1')(\partial^\mu \phi_1') - \frac{1}{2}\cdot\ 2\mu^2\phi_1'\phi_1' \\ &- \frac{1}{4}(F^{\mu\nu}F_{\mu\nu}) + \frac{1}{2}\cdot\ e^2\phi_0^2 A_\mu A^\nu \\ &+ \phi_0 e^2 \phi_1' A_\mu A^\mu + \frac{1}{2}e^2\phi_1'^2 A_\mu A^\mu + \mathcal{O}(\phi'^3)...\end{aligned} \tag{2.40}$$

The degree of freedom that ϕ_2 represents, is absorbed as a longitudanal polarization of the A_{mu} field, a forbidden for massless guage bosons, but necessary for massive bosons.

For this case of an abelian symmetry $U(1)$, it was shown that if a complex scalar field, which interacts with itself and another vector field, can gains a non-zero vacuum expectation value. The Lagrangian can be expanded about this new mimimum, generating a mass term for the vector field. One of the degrees of freedom of the orginial complex scalar field is then absorbed as a longitudanal polarization state of the massive vector field.

2.5 The Higgs Mechanism in a non-Abelian Theory

Before describing the elctroweak guage theory of $SU(2)\otimes U(1)$, it will be helpful to see the effects of the Higgs mechanism for the non-Abelian group, $SU(2)$ by itself. Consider an an example of an $SU(2)$ gauge field coupled to a scalar field that transforms like a real-valued vector under $SU(2)$ transformations [3]. The field ϕ will have the form:

$$\phi = \begin{pmatrix}\phi_1 \\ \phi_2 \\ \phi_3\end{pmatrix} \tag{2.41}$$

where the components, ϕ_i are real-valued fields. The $SU(2)$ transformation for this scalar field will also look like:

$$\phi \rightarrow e^{i\alpha^i T^i}\phi \tag{2.42}$$

where the matrices, T^i are defined as:

$$iT^1 = \begin{pmatrix}0 & 0 & 0 \\ 0 & 0 & 1 \\ 0 & -1 & 0\end{pmatrix},\ T^2 = \begin{pmatrix}0 & 0 & -1 \\ 0 & 0 & 0 \\ 1 & 0 & 0\end{pmatrix},\ T^3 = \begin{pmatrix}0 & 1 & 0 \\ -1 & 0 & 0 \\ 0 & 0 & 0\end{pmatrix} \tag{2.43}$$

The Lagrangian for this field will feature a Higgs potential term along with the previously mentioned $SU(2)$ guage fields, A_μ^a coupled to the scalar field, phi, and is given by:

$$\mathcal{L} = -\frac{1}{4}F_{\mu\nu}^a F^{a\mu\nu} + |D_\mu\phi|^2 + \mu^2\phi^*\phi - \frac{\lambda}{4}(\phi^*\phi)^2 \tag{2.44}$$

where $F_\mu\nu^a$, the field strength tensor is defined as:

$$F^a_{\mu\nu} = (\partial_\mu A^a_\nu - \partial_\nu A^a_\mu) + g\epsilon^{abc} A^b_\mu A^c_\nu \tag{2.45}$$

and the covariant derivative is defined as:

$$D_\mu = (\partial_\mu + igA^a_\mu T^a)\phi \tag{2.46}$$

Similarly to the Abelian case, the Higgs potential will induce a spontaneous symmetry breaking, and one of the components of the field ϕ will gain a vacuum expectation value. After this breaking and expanding around the ground state potential, the field ϕ will have the form:

$$\phi = \frac{1}{\sqrt{2}} \begin{pmatrix} 0 \\ 0 \\ v+h \end{pmatrix} \tag{2.47}$$

There has been no loss in generality in assuming this form since, similarly to the abelian case, we can use the gauge symmetry of $SU(2)$ to rotate the field into this configuration. Goldstone's theorem tells us that we should expect two massive gague bosons corresponding to the T^1, and T^2 generators, while the T^3 generator will correspond to a massless gauge boson, since ϕ is still invariant under T^3 transformations.

As in the Abelian case, the mass terms for the gauge bosons are generated from the covariant derivative term, $|D_\mu \phi|^2$

$$\begin{aligned}
D_\mu \phi &= \frac{1}{\sqrt{2}} \left(\partial_\mu + gA^1_\mu \begin{pmatrix} 0 & 0 & 0 \\ 0 & 0 & 1 \\ 0 & -1 & 0 \end{pmatrix} + gA^2_\mu \begin{pmatrix} 0 & 0 & -1 \\ 0 & 0 & 0 \\ 1 & 0 & 0 \end{pmatrix} + gA^3_\mu \begin{pmatrix} 0 & 1 & 0 \\ -1 & 0 & 0 \\ 0 & 0 & 0 \end{pmatrix} \right) \begin{pmatrix} 0 \\ 0 \\ v+h \end{pmatrix} \\
&= \frac{1}{\sqrt{2}} \begin{pmatrix} 0 \\ 0 \\ \partial_\mu \end{pmatrix} + \frac{gA^1_\mu}{\sqrt{2}} \begin{pmatrix} 0 \\ v+h \\ 0 \end{pmatrix} - \frac{gA^2_\mu}{\sqrt{2}} \begin{pmatrix} v+h \\ 0 \\ 0 \end{pmatrix} \\
&= \frac{1}{\sqrt{2}} \begin{pmatrix} g(v+h)A^1_\mu \\ g(v+h)A^2_\mu \\ \partial_\mu h \end{pmatrix}
\end{aligned} \tag{2.48}$$

Therefore

$$|D_\mu\phi|^2 = \frac{1}{2}\partial_\mu h\partial^\mu h + \frac{g^2v^2}{2}\left((A^1_\mu)^2 + (A^2_\mu)^2\right) + \frac{g^2}{2}(h^2+2hv)\left((A^1_\mu)^2 + (A^2_\mu)^2\right) \tag{2.49}$$

This theory produces two massive bosons, A^1_μ and A^2_μ, both with mass, $m_A = gv$. These fields have h, and h^2 couplings to the Higgs boson. The third guage field, A^3_μ, remains massles and is not coupled to the Higgs field. This model is beginning to resemble a description of electroweak physics, however, a third massive boson is necessary, as is a new gague symmetry in order to generate it. That is the subject of the next section.

2.6 Glashow Weinberg Salam Theory

Glashow, Weinberg, and Salam published their theory unifying elctromagnetic and weak forces in the 1960s [14] [15] [16]. It begins with the requirement of a $SU(2)_L \otimes\ U(1)$ symmetry and incorporates the Higgs mechanism to give mass to the guage bosons of the weak force. As described earlier, the $U(1)$ symmetry requires introducing a vector field, which will be labeled B_μ, and an interaction term, which is absorbed into the covariant derivative, D_μ. The transformation will also be paramaterized with a with a quantum number, Y, known as hypercharge. The $SU(2)$ symmetry requires the introduction of three new vector fields, which will be labeled $W^i_\mu, i = 1, 2, 3$. The quantum number associated with this gauge group is known as isospin, and is determined by the T^3 operator, acting on an $SU(2)$ doublet on the third generator of the group. The $SU(2)\otimes\ U(1)$ transformation, $U(x)$, will then be give by:

$$U(x) = e^{i\alpha^a(x)\tau^a}e^{iY\alpha(x)/} \tag{2.50}$$

where $\tau^a = \sigma^a/2$, the Pauli matrices, 2.18. These gauge fields will be coupled, via the covariant derivative, to a doublet of complex scalar fields ϕ, with hypercharge $Y = +1/2$. A Higgs potential will be added to generate the spontaneous symmetry breaking that will give mass to three of the guage fields, and leave one massless. In order to preserve the $SU(2)_L\otimes\ U(1)$ symmetry, the new covariant derivative will take the form:

$$D_\mu = (\partial_\mu - igW^a_\mu\tau^a - \frac{i}{2}g'B_\mu) \tag{2.51}$$

The subscript L on $SU(2)_L$ refers to the experimental results that the weak force violates parity maximally, by only interacting with the left-handed chiral component of a field. Right versus left chiralty is determined by whether the spin of a particle is aligned or anti-aligned with its direction of motion, and in general a particle is represented by a linear combination of its right and left handed components. This idea was first proposed by Chen Ning Yang and Tsung-Dao Lee, in the 1950s. Their ideas were validated by the experimental discovery of partiy violation in 1957, through the beta decays of Cobalt 60 atoms by C.S Wu. That same year, Yang and Lee were awrded the nobel prize for their insight [17]. In this model, then, the left-handed components of the particles participate in the weak interaction and are formed into doublets, while the right handed components are singlets, and will only interact with the electromagnetic field, B_μ. The quantum numbers of the doublet will be given by $+1/2$ for the upper component of the $SU(2)$ doublet, and -1/2 for the lower component. The fermion content of this theory is then given by:

$$\begin{gathered}\begin{pmatrix}\nu_L \\ e_L\end{pmatrix}, e_R \\ \begin{pmatrix}u_L \\ d_L\end{pmatrix}, u_R, d_R\end{gathered} \tag{2.52}$$

where the right handed neutrino, ν_R has been ommited, since it has zero charge, and isospin, and therefore does not participate in any of the interactions of this theory. The complete Lagrangian is given by a sum of free particle terms for massless bosons, fermions, and Higgs scalar fields; the Higgs potential; and a Yukawa coupling term between the fermions and the Higgs, which generates their masses.

$$\mathcal{L}_{GWS} = \mathcal{L}_{BosonKE} + \mathcal{L}_{Higgs} + \mathcal{L}_{FermionKE} + \mathcal{L}_{Yukawa} \tag{2.53}$$

The Higgs potential will have the form:

$$\mathcal{L}_{Higgs} = (D_\mu \phi)^\dagger (D^\mu \phi) + \mu^2 \phi^\dagger \phi - \lambda(\phi^\dagger \phi)^2 \tag{2.54}$$

The Higgs potential will break the symmetry of the Lagrangian when one of the four degrees of freedom in the complex scalar doublet, ϕ, spontaneously acquires a vacuum expectation value. In this case, it will generate three massive gauge bosons, one massless gauge boson, and a massive scalar field. After gaining a vacuum expectation value, and expanding about this value, the scalar fields will have the form:

$$\langle \phi \rangle = \frac{1}{\sqrt{2}} \begin{pmatrix} 0 \\ v + h \end{pmatrix} \tag{2.55}$$

where no loss of generality has occured since we are always able to rotate into this form through the appropriate gauge transformations, similar to what was descibed in the Abelian case. It should also be noted that this form is not invariant to any of the individual generators t^a, however ϕ will be invariant to a combination of $T^3 + Y$ generators. Per Goldstone's thereom, we should expect this linear combination of fields to be the massless vector boson after symemtry breaking. The massless eigenstate will be the electromagnetic field, $A_\mu \sim A^3_\mu + B_\mu$. The electric charge quantum number, Q, is then defined as

$$Q = T^3 + Y \tag{2.56}$$

As before, the generation of the masses for the guage bosons are generated by the interaction of their fields with the Higgs field via the covariant derivative.

$$D_\mu\phi = \frac{1}{\sqrt{2}}\left(\partial_\mu - \frac{ig}{2}A^1_\mu\begin{pmatrix}0 & 1\\ 1 & 0\end{pmatrix} - \frac{ig}{2}A^2_\mu\begin{pmatrix}0 & -i\\ i & 0\end{pmatrix} - \frac{ig}{2}A^3_\mu\begin{pmatrix}1 & 0\\ 0 & -1\end{pmatrix}\right)\begin{pmatrix}0\\ v+h\end{pmatrix} \tag{2.57}$$

$$= \frac{1}{\sqrt{2}}\begin{pmatrix}(\frac{g}{2}(v+h)A^2_\mu) + i(\frac{g}{2}(v+h)A^1_\mu)\\ \partial_\mu + i(\frac{1}{2}(v+h)(gA^3_\mu - g'B_\mu))\end{pmatrix}$$

Taking the dot product of this with its hermitian conjugate gives the $|D_\mu\phi|^2$ term:

$$\begin{aligned}|D_\mu\phi|^2 =& \frac{1}{2}\partial_\mu h\partial^\mu h + \frac{1}{2}\frac{g^2v^2}{4}((A^1_\mu)^2 + (A^2_\mu)^2) + \frac{v^2}{4}(gA^3_\mu - g'B_\mu)^2\\ &+ \frac{1}{2}g^2 4(h^2 + 2vh)((A^1_\mu)^2 + (A^2_\mu)^2) + \frac{1}{2}\frac{1}{4}(h^2 + 2vh)(gA^3_\mu - g'B_\mu)\end{aligned} \tag{2.58}$$

From equation 2.58 we can identify three massive and one massless guage bosons, corresponding the the charged and nuetral weak currents, and the elctromagnetic current.

$$\begin{aligned}W^\pm_\mu &= \frac{1}{\sqrt{2}}(A^1_\mu \mp iA^2_\mu) && \text{with mass } m_W = g\frac{v}{2};\\ Z^0_\mu &= \frac{1}{\sqrt{g^2+g'^2}}(gW^3_\mu - g'B_\mu) && \text{with mass } m_Z = \frac{v}{2}\sqrt{g^2+g'^2};\\ A_\mu &= \frac{1}{\sqrt{g^2+g'^2}}(gW^3_\mu + g'B_\mu) && \text{with mass } m_A = 0;\end{aligned} \tag{2.59}$$

where the last field, A_μ is absent from the covariant derivative term, but already identified as the massless gauge boson of the theory due to it's gauge invariance under a $T^3 + Y$ rotation. Using these definitions the covariant derivative has the following form:

$$\begin{aligned}D_\mu =& \partial_\mu - \frac{ig}{\sqrt{2}}(W^+T^+ + W^-T^-)\\ &- \frac{i}{\sqrt{g^2+g'^2}}Z^0_\mu(gT^3 - g'Y) - \frac{gg'}{\sqrt{g^2+g'^2}}A_\mu(T^3+Y)\end{aligned} \tag{2.60}$$

where $T^\pm = \frac{1}{2}(\sigma^1 \pm \sigma^2)$. From this form, we can identiy the fundamental electric charge, e, as

$$e = \frac{gg'}{\sqrt{g^2 + g'^2}} \tag{2.61}$$

The similarity in the forms between Z^0_μ and A_μ suggest that their relationship can be expressed in a simpler form, as the rotation of underlying guage fields A^3_μ and B_μ through the weak mixing angle, θ_W

$$\begin{pmatrix} Z^0_\mu \\ A_\mu \end{pmatrix} = \begin{pmatrix} \cos\theta_W & -\sin\theta_W \\ \sin\theta_W & \cos\theta_W \end{pmatrix} \begin{pmatrix} A^3_\mu \\ B_\mu \end{pmatrix} \tag{2.62}$$

where $\tan\theta_W = \frac{g'}{g}$. Expanding 2.62, we have the definitions of the Z^0_μ and A_μ fields in terms of θ_W

$$\begin{aligned} Z^0_\mu &= A^3_\mu \cos\theta_W - B_\mu \sin\theta_W \\ A_\mu &= A^3_\mu \sin\theta_W + B_\mu \cos\theta_W \end{aligned} \tag{2.63}$$

The weak mixing angle, θ_W, also provides a simple relationship between the $W^\pm_\mu$ and Z^0_μ fields:

$$m_W = m_Z \cos\theta_W \tag{2.64}$$

The covariant derivative, D_μ is also rewritten in terms of the mass eignenstates of the gauge fields

$$D_\mu = (\partial_\mu - \frac{ig}{\sqrt{2}}(W^+_\mu + W^-_\mu T^-) - \frac{ig}{\cos\theta_W} Z^0_\mu (T_3 - sin^2\theta_W Q) - ieA_\mu Q) \tag{2.65}$$

where $g = e/\cos\theta_W$. The square of the covariant derivative is then written as

$$\begin{aligned} |D_\mu|^2 = &\frac{1}{2}\partial_\mu h \partial^\mu h + \frac{1}{2} m^2_W W^+_\mu W^{\mu +} + \frac{1}{2} m^2_W W^-_\mu W^{\mu -} + \frac{1}{2} m^2_Z Z^0_\mu Z^{\mu 0} \\ &+ (\frac{h^2}{v^2} + \frac{h}{v})[\frac{1}{2} m^2_W (W^+_\mu W^{\mu +} + W^-_\mu W^{\mu -}) + \frac{1}{2} m^2_Z Z^0_\mu Z^{\mu 0}] \end{aligned} \tag{2.66}$$

With the form of the covariant derivative in place, the fermionic kinematic term of the Lagrangian can be described. As mentioned earlier, the masses of the fermions in the model will be generated by the Yukawa interaction term with the Higgs, so this term only involves the covariant derivatives acting on the left-handed doublet and right-handed singlet states of this model.

The quantum number assignments for the leptons, which are chosen in order to reproduce the known values of their electric charges, are shown in table 2.1. The values of these quantum

	ν_L	e_L	e_R	u_L	d_L	u_R	d_R
Isospin	+1/2	-1/2	0	+1/2	-1/2	0	0
Hypercharge	-1/2	-1/2	-1	+1/6	1/3	2/3	-1/3
Electric Charge	0	-1	-1	2/3	-1/3	2/3	-1/3

Table 2.1: The quantum numbers Isospin and Hypercharge are assigned for each of the $SU(2)$ and $U(1)$ symmetries respectively

numbers enter into the covariant derivative via the Z^0_μ term of equation 2.65. The fermionic kinetic energy term of the Lagrangian is given by:

$$\begin{aligned} \mathcal{L}_{Fermion} = & \bar{E}_L(i\gamma^u D_\mu)E_L + \bar{e}_R(i\gamma^u D_\mu)e_R \\ & \bar{Q}_L(i\gamma^u D_\mu)Q_L + \bar{u}_R(i\gamma^u D_\mu)u_R + \bar{d}_R(i\gamma^u D_\mu)d_R \end{aligned} \tag{2.67}$$

Expanding the covariant term for the left-handed electron shows its explicit coupling to the guage boson fields.

$$\begin{aligned} \mathcal{L}_{E_L} = & \begin{pmatrix} \bar{\nu_L} & \bar{e_L} \end{pmatrix} \left((i\gamma^\mu(\partial_\mu - \frac{ig}{\sqrt{2}}(W^+_\mu T^+ + W^-_\mu T^-) - \frac{ig}{\cos\theta_W} Z^0_\mu(T^3 - \sin^2\theta_W Q) - ieA_\mu Q)\ ) \right) \begin{pmatrix} \nu_L \\ e_L \end{pmatrix} \\ = & \bar{\nu_L} i\gamma^\mu\partial_\mu\nu_L + \bar{e_L} i\gamma^\mu\partial_\mu e_L + \frac{ig}{\sqrt{2}} W^+_\mu \bar{\nu_L}\gamma^\mu e + \frac{ig}{\sqrt{2}} W^-_\mu \bar{e_L}\gamma^\mu\nu_L \\ & + \frac{ig}{\cos\theta_W}\bar{\nu_L}(1/2)\gamma^\mu\nu_L + \frac{ig}{\cos\theta_W}\bar{e_L}\gamma^\mu(-1/2 + \sin^2\theta_W(+1))e_L + (ie)\bar{e_L}\gamma^\mu A_\mu(-1) \end{aligned} \tag{2.68}$$

All of the terms will be combined with the final, spontaneously broken GWS Lagranian at the end of this section.

The final term to discuss in the theory, before combing all of the results, is the Yukawa interaction term between the fermion fields and the Higgs. For the electron, this term takes the form:

$$\begin{aligned} \mathcal{L}_{Yukawa} = & -\lambda_e \bar{E_L}\cdot\phi\ e_R - \lambda_e E_L\cdot\phi\ \bar{e_R} \\ = & -\frac{\lambda_e}{\sqrt{2}}(v+h)(\bar{e_L}e_R + e_L\bar{e_R}) \\ = & --\frac{\lambda_e v}{\sqrt{2}}(\bar{e_L}e_R + e_L\bar{e_R}) + -\frac{\lambda_e}{\sqrt{2}}(\bar{e_L}e_R + e_L\bar{e_R})h \end{aligned} \tag{2.69}$$

where the mass of the electron is identified as $m_e = \frac{\lambda_e v}{\sqrt{2}}$. In order to generate the masses of the particles, each fermion has its own unique λ value. So while the Higgs mechanism is able to generate the masses in a way that preserves the underlying $SU(2) \otimes U(1)$ symmetry, it does not explain the heirarchy of masses since each λ value is unique to each lepton. The second term in last equation of 2.69 is the coupling of the Higgs particle, h, to the fermions. The coupling is proportional to the mass of the particle. The largest of these is to the top quark, with $m_t = 73.21 \pm 0.51 \pm 0.71 GeV$.

The Yuakawa coupling for the quarks is necessarily modified when additional quarks besides the u and d are added to the theory. This is because there can be additional coupling terms that mix generations. This occurs when the mass eigenstate of the quarks is not the same as the interaction eigenstate. The modification requires the expansion of the u_L and d_L components into a vector of left handed quarks. If we let

$$u_L^i = (u_L, c_L, t_L), \quad d_L^i = (d_L, s_L, b_L) \tag{2.70}$$

represent the up and down-type quarks in the orginal weak interaction basis, then the vectors, u_L^i' and d_L^i', can be defined as the diagonlized basis for the Higgs coupling. They are related through a unitary transformation.

$$u_L^i = U_u^{ij} u_L^{j\prime}, \quad d_L^i = U_d^{ij} d_L^{j\prime} \tag{2.71}$$

The interaction terms with the charged gauge boson currents must then be rewritten as

$$J_W^{\mu +} = \frac{1}{\sqrt{2}} \bar{u_L^i} \gamma^\mu d_L^i = \frac{1}{\sqrt{2}} \bar{u_L^{i\prime}} \gamma^\mu (U_u^\dagger U_d) d_L^{j\prime} = \frac{1}{\sqrt{2}} \bar{u_L^{i\prime}} \gamma^\mu V_{ij} d_L^{j\prime} \tag{2.72}$$

where V_{ij} is the 3x3 Cobibbo-Kobayashi-Maskawa (CKM) matrix describing the mixing among six quarks [18] [19]. It is an extension of the Glashow-Iliopoulos-Maiaini mechanism, which was a 2x2 matrix that predicted the existence of a fourth quark, the charm quark. The GIM mechanism was an attempt to suppress flavor-changing-neutral currents, which occur at LO in a three-quark model, but not in a four-quark model. The CKM matrix, however, was motivated by an attempt to explain CP violation in the weak interaction. At the time of its publication, the bottom and top quarks were not predicted. After these were discovered, they were awarded the nobel prize in physics in 2008.

At this point, all the of the pieces are ready to write down the GWS Lagrangian, after the Higgs mechanism has spontaneously broken the $SU(2) \otimes U(1)$ symmetry.

$$\begin{aligned} \mathcal{L}_{Unbroken} = & -\frac{1}{4} A_{\mu\nu}^a A^{\mu\nu\ a} - \frac{1}{4} F_{\mu\nu} F^{\mu\nu} \\ & + |D_\mu \phi|^2 + \mu^2 (\phi^\dagger \phi) - \lambda (\phi^\dagger \phi)^2 \\ & + \bar{E_L} (i \gamma^\mu D_\mu) E_L + \text{ similar terms for } e_R, U_L, u_R, d_R \\ & - \lambda_e \bar{E_L} \cdot \phi \ e_R + h.c. + \text{ similar terms for } e_R, U_L, u_R, d_R \end{aligned} \tag{2.73}$$

$$
\begin{aligned}
\mathcal{L}_{GWS} = & -\frac{1}{4}(Z^0_{\mu\nu})^2 - \frac{1}{2}(W^+_{\mu\nu}W^-_{\mu\nu}) - \frac{1}{4}(F_{\mu\nu})^2 \\
& + ig\cos\theta_W \left((W^-_\mu W^+_\nu - W^-_\nu W_\mu)\partial^\mu Z^{0\nu} + W^+_{\mu\nu}W^{-\mu}Z^{0\nu} + W^-_{\mu\nu}W^{+\mu}Z^{0\nu}\right) \\
& + ie\left((W^-_\mu W^+_\nu - W^-_\nu W^+_\mu)\partial^\mu A^\nu + W^+_{\mu\nu}W^{-\mu}A^\nu - W^-_{\mu\nu}W^{+\mu}A^\nu\right) \\
& + g^2\cos^2\theta_W\left(W^+_\mu W^-_\nu Z^{0\mu}Z^{0\nu} - W^+_\mu W^{-\mu}Z^0_\nu Z^{0\nu}\right) \\
& + g^2\left(W^+_\mu W^-_\mu A^\mu A^\nu - W^+_\mu W^{-\mu}A_\nu A^\nu\right) \\
& + ge\cos\theta_W\left(W^+_\mu W^-_\nu(Z^{0\mu}A_\nu + Z^{0\nu}A^\mu) - 2W^+_\mu W^{-\mu}A^\nu\right) \\
& + \frac{1}{2}g^2(W^+_\mu W^-_\nu)(W^{+\mu}W^{-\nu} - W^{+\nu}W^{-\mu}) \\
& + \frac{1}{2}\partial_\mu h\partial^\nu h - v^2\lambda h^2 + \frac{1}{2}m^2_W W^+_\mu W^{+\mu} + \frac{1}{2}m^2_W W^-_\mu W^{-\mu} + \frac{1}{2}m^2_Z Z^0_\mu Z^{0\mu} \\
& + (\frac{h^2}{v^2} + \frac{h}{v})\left(\frac{1}{2}m^2_W(W^+_\mu W^{+\mu} + W^-_\mu W^{-\mu}) + \frac{1}{2}m^2_Z Z^0_\mu Z^{0\mu}\right) - \lambda v h^3 - \frac{1}{4}\lambda h^4 \\
& + \bar{E_L}(i\gamma^\mu\partial_\mu)E_L + \bar{e_R}(i\gamma^\mu\partial_\mu)e_R + \bar{Q_L}(i\gamma^\mu\partial_\mu)Q_L + \bar{u_R}(i\gamma^\mu\partial_\mu)u_R + \bar{d_R}(i\gamma^\mu\partial_\mu)d_R \\
& + g(W^+_\mu J^{\mu+}_W + W^-_\mu J^{\mu-}_W + Z^0_\mu J^\mu_Z) + eA_\mu J^\mu_{EM} \\
& - \frac{\lambda_e v}{\sqrt{2}}(\bar{e_L}e_R + \bar{e_R}e_L) + -\frac{\lambda_e h}{\sqrt{2}}(\bar{e_L}e_R + \bar{e_R}e_L) \\
& - \frac{\lambda_u v}{\sqrt{2}}(\bar{u_L}u_R + \bar{u_R}u_L) + -\frac{\lambda_u h}{\sqrt{2}}(\bar{u_L}u_R + \bar{u_R}u_L) \\
& - \frac{\lambda_d v}{\sqrt{2}}(\bar{d_L}d_R + \bar{d_R}d_L) + -\frac{\lambda_d h}{\sqrt{2}}(\bar{d_L}d_R + \bar{d_R}d_L)
\end{aligned} \tag{2.74}
$$

where the currents of the electroweak interaction, $J^{\mu+}_W$, $J^{\mu-}_W$, J^μ_Z, J^μ_A are defined as:

$$
\begin{aligned}
J^{\mu+}_W &= \frac{1}{\sqrt{2}}\left(\bar{\nu_L}\gamma^\mu e_L + \bar{u^{i\prime}_L}\gamma^\mu V_{ij}d^{j\prime}_L\right) \\
J^{\mu-}_W &= \frac{1}{\sqrt{2}}\left(\bar{e_L}\gamma^\mu \nu_L + \bar{d^{i\prime}_L}\gamma^\mu V_{ij}u^{j\prime}_L\right) \\
J^\mu_Z &= \frac{1}{\cos\theta_W}(\bar{\nu_L}\gamma^\mu(+1/2)\nu_L + \bar{e_L}\gamma^\mu(-1/2+\sin^2\theta_W)e_L + \bar{e_R}\gamma^\mu\sin^2\theta_W e_R \\
&\quad + \bar{u_L}\gamma^\mu(1/2 - 2/3sin^2\theta_W)u_L + \bar{u_R}\gamma^\mu(-2/3sin^2\theta_W)u_R \\
&\quad + \bar{d_L}\gamma^{mu}(-1/2 + 1/3sin^2\theta_W)d_L + \bar{d_R}\gamma^\mu(1/3sin^2\theta_W)d_R) \\
J^\mu_{EM} &= \bar{e_{L,R}}\gamma^\mu(-1)e_{L,R} + \bar{u_{L,R}}\gamma^\mu(2/3)u_{L,R} + \bar{d_{L,R}}\gamma^\mu(-2/3)d_{L,R}
\end{aligned} \tag{2.75}
$$

383 2.7 The Standard Model of Particle Physics

The Standard Model of particle physics, extends the GWS model by incorporating the QCD interaction between the quarks and gluons. The symmetry of this theory is that of:

$$SU(3)_C \otimes\ SU(2)_L \otimes\ U(1)_\gamma \tag{2.76}$$

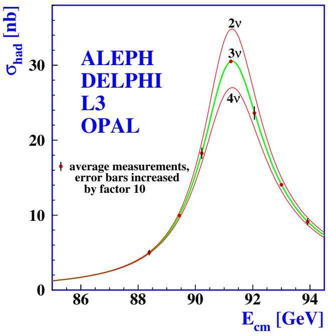

(a) Measurement of the width of Z boson from LEP, comparing the hypotheses of 2, 3, or 4 neutrino generations

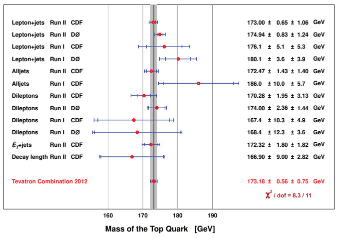

(b) Measurement of the top mass from the CDF detector at the Tevatron

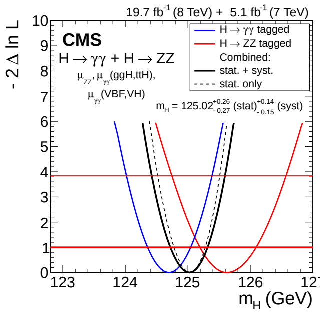

(c) Measurement of the Higgs mass from the CMS detector at the LHC

Figure 2.4: Experimental milestones of the Standard Model

The Lagrangian of the model is given by

$$\mathcal{L}_{SM} = \mathcal{L}_{GWS} - \frac{1}{4} G^a_{\mu\nu} G^{a\mu\nu} + g_S C^a_\mu J^{a\mu}_{QCD} \tag{2.77}$$

where the current for the QCD interaction, $J^{a\mu}_{QCD}$ is defined as:

$$J^a_{QCD} = \bar{u}^i \gamma^\mu t^a u^i + \bar{d}^i \gamma^\mu t^a d^i \tag{2.78}$$

where t^a are the Gell-Mann matrices defined in equation 2.30. The field strength tensor for the eight gluon fields, $G^a_{\mu\nu}$, is defined as

$$G^a_{\mu\nu} = (\partial_\mu C^a_\nu - \partial_\nu C^a_\mu) - g_S f^{abc} C^b_\mu C^c_\mu \tag{2.79}$$

The experimental evidence in favor of the SM is compelling. It has not only been able to describe existing phenomenon to great precision, but has also predicted the existence of new forms of matter and interactions among fundamental particles. The UA1 [20] [21] and UA2 [22] [23] experiments at CERN, under the leadership of Carlo Rubbia, discovered the W and Z bosons in 1983. The experiments observed a handful of events, in $p\bar{b}$ collisions, at $\sqrt{s} = 540\,\text{GeV}$, and were able to measure the masses to be $M_W \sim 80\,\text{GeV}$ and $M_Z \sim 95\,\text{GeV}$.

In the following years, from 1989-2000, the Large electron-positron (LEP) collider at CERN conducted precision measurments of the Standard Model [24] [25]. Along with high-precision measurements on on the W, Z masses:

$$\begin{aligned} m_Z &= 91.1875 \pm 0.0021\,\text{GeV} \\ m_W &= 80.376 \pm 0.0033\,\text{GeV} \end{aligned} \tag{2.80}$$

the experiment was also able to put stringent limits on the existence of more than three families of leptons and quarks by measuring the width of the Z boson. Figure 2.4(a) shows the comparison of two, three, and four family hypotheses to data.

Another milestone for the Standard Model occured in 1995 when the CDF [26] and D0 experiments [27] at the Tevatron announced the observation of the top quark, with $m_t \sim 176$ GeV, in $p\bar{p}$ collisions at $\sqrt{s} = 1.8$ TeV. Figure 2.4(c) shows a plot from 2012, the latest top quark mass measurements from CDF, which reports a $m_t = 173.18 \pm 0.56 \pm 0.75$ GeV. It was the last quark predicted by the CKM matrix to be observed, and earned Makoto Kobayashi and Toshihide Maskawa the nobel prize in 2008 for their work extending the quark sector to three families and parameterizing their electroweak mixing.

Yet another milestone was reached in 2012, when the CMS and ATLAS detectors at CERN anounced the observation of a new boson, with characteristics strikingly similar to the elusive Higgs boson of the SM. Figure 2.4(c) shows the latest measurement results on the mass from the $H \to \gamma\gamma$ and $H \to ZZ$ channels, with a $m_H = 125.02 \pm 0.27 \pm 0.15$. One of the most important remaining goals is to measure the couplings of this new boson to all of the other particles in the Standard Model. Of particular interest is the coupling to the top-quark, since it offers the largest value of the Higgs Yukawa coupling to measure. This offers a test of the nature of the coupling, as well as a probe into deviations from its value.

2.8 Higgs Procution in pp Collisions at the LHC

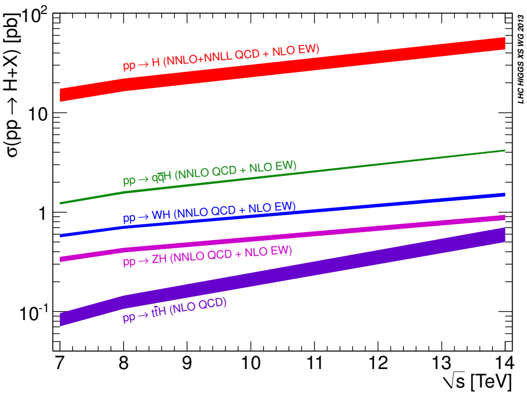

Figure 2.5: Higgs production cross-sections at the LHC, for 7-14 TeV pp collisions

The rest of the thesis will describe the search for Higgs boson production in proton-proton collisions at the LHC, so it will be useful to understand the production mechanisms for the Higgs in this scenario. At the LHC collision energies $7 - 14$ TeV, there are four dominant production mechanisms that produce Higgs events: gluon-gluon fusion (ggf), vector-boson fusion (vbf), associated production with vector bosons (VH), and associated production with top-quark pairs (ttH). Figure 2.5 shows the relative cross sections for each of these mechanisms.

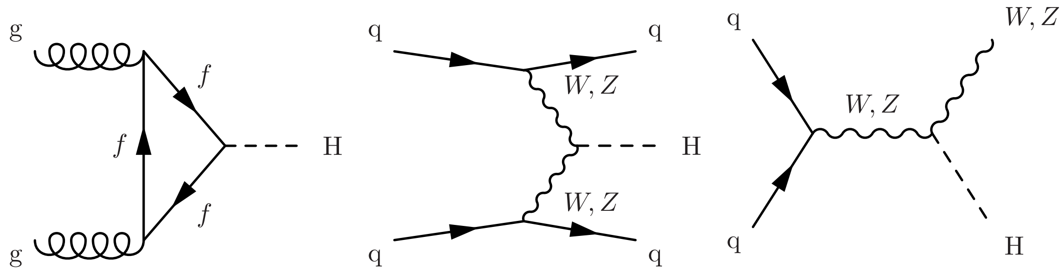

(a) Gluon-Gluon Fusion (b) Vector Boson Fusion (c) Associated Production with W, Z

Figure 2.6: Feynman diagrams for the three largest Higgs production modes at the LHC

Gluon-gluon fusion, which proceeds via a heavy quark loop [28], is the dominant production mechanism at the LHC. The QCD radiative corrections to the total cross section have been computed at the next-to-leading order (NLO) and at the next-to-next-to-leading order (NNLO accuracy). The cross section for Higgs production at $m_H = 125\,\text{GeV}$ and $\sqrt{s} = 8\,\text{TeV}$, the cross section is given as:

$$\sigma_{ggF} = 19.27 \quad \pm \quad \text{QCD Scale Unc.}^{+7.2\%}_{-7.8\%} \quad \pm \quad \text{PDF+}\alpha_S \text{ Unc.}^{+7.4\%}_{-6.9\%} \quad \text{pb}^{-1} \tag{2.81}$$

Figure 2.6(a) shows a Feynman diagram for this process. The triangle loop contains all strongly coupled fermions, which is dominated by the top-quark since the Yukawa coupling to the Higgs is the largest.

Vector boson fusion proceeds through the fusion of W^+W^- or Z^0Z^0 gauge bosons [28]. The characteristic signature of the production mode is the associated production of two quarks, typically at a low angle relative to the proton beam. This process has been caclulated to NNLO for QCD and NLO for Electroweak corrections [28]. The cross section at $m_H = 125\,\text{GeV}$ and $\sqrt{s} = 8\,\text{TeV}$ is given as:

$$\sigma_{VBF} = 1.653 \quad \pm \quad \text{EW Unc.}^{+4.5\%}_{-4.5\%} \quad \pm \quad \text{QCD Scale Unc.}^{+0.2\%}_{-0.2\%} \quad \pm \quad \text{PDF+}\alpha_S \text{ Unc.}^{+2.6\%}_{-2.8\%} \quad \text{pb}^{-1} \tag{2.82}$$

Figure 2.6(b) shows a Feynman diagram for VBF production. The large coupling to the W, Z bosons helps to make this the sub-dominant production mechanism at the LHC. However, the gluon content of the proton at TeV energies is much larger than that of the valence quarks, thus the relative suppression.

The third largest production mechanism for Higgs bosons at the LHC is through associated production with a W or Z boson [28]. It has been calculated to NNLO for QCD and NLO for Electroweak corrections. This process is also sometimes referred to as, Higgstrahlung, since it resemble the bremstrahlung process of an electron radiating a photon. The higher order electroweak corrections are similar to that of the Drell-Yan, so much of the technology to compute the cross-section can be borrowed from existing EW calculations. The cross section for $m_H = 125\,\text{GeV}$ and $\sqrt{s} = 8\,\text{TeV}$ is:

$$\begin{aligned}\sigma_{WH} &= 0.7046 \quad \pm \quad \text{QCD Scale Unc.}^{+1.0\%}_{-1.0\%} \quad \pm \quad \text{PDF}+\alpha_S \text{ Unc.}^{+2.3\%}_{-2.3\%} \quad \text{pb}^{-1} \\ \sigma_{ZH} &= 0.4153 \quad \pm \quad \text{QCD Scale Unc.}^{+3.1\%}_{-3.1\%} \quad \pm \quad \text{PDF}+\alpha_S \text{ Unc.}^{+2.5\%}_{-2.5\%} \quad \text{pb}^{-1}\end{aligned} \tag{2.83}$$

Figure 2.6(c) shows the Feynman diagram for VH production. This channel is most useful for identifying hadronic decays of the Higgs, since the associated gague boson can decay to leptons, giving a strong kinematic handle over backgrounds that would normally overwhelm a similar search in the ggF channel.

2.9 $t\bar{t}H$Production in pp Collisions at the LHC

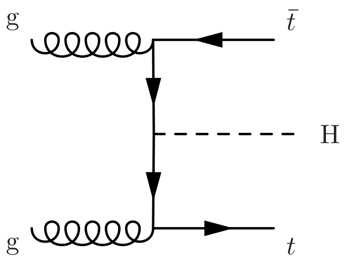

Figure 2.7: Feynman diagram for $t\bar{t}H$production

The $t\bar{t}H$production mode is the fourth largest production mode at the LHC [28]. This production mode has been calculated to NLO in QCD [29] [30] and has been studied recently with the state of the art NLO tools using the aMC@NLO [31] and POWHEG (PYTHIA+HERWIG) [32] frameworks. Studies have also been performed interfacing NLO QCD studies [33] with the Sherpa parton shower framework [34]. Additional studies on the effects of spin correlations with the aMC@NLO and Madspin framework have also been performed [35].

It has been found that the additional of NLO effects increases the cross-section relative to LO by $\sim 20\%$. The largest theoretical uncertainty comes from the variation of the renormalization and factorization scale, the QCD coupling α_S, and the PDF uncertainty. The renomarlization and factorization scales are set to $\mu_R = \mu_F = (1/2)(m_T + m_T + m_H)$ and are varied by a factor of 2 to determine the cross-section's dependence on these parameters. Three different PDF sets, MSTW2008, CTEQ6.6, and NNPDF2.0 were used with the appropriate corresponding values of α_S to determine the combined effect of varying PDF+α_S. The cross section for $m_H = 125\,\text{GeV}$

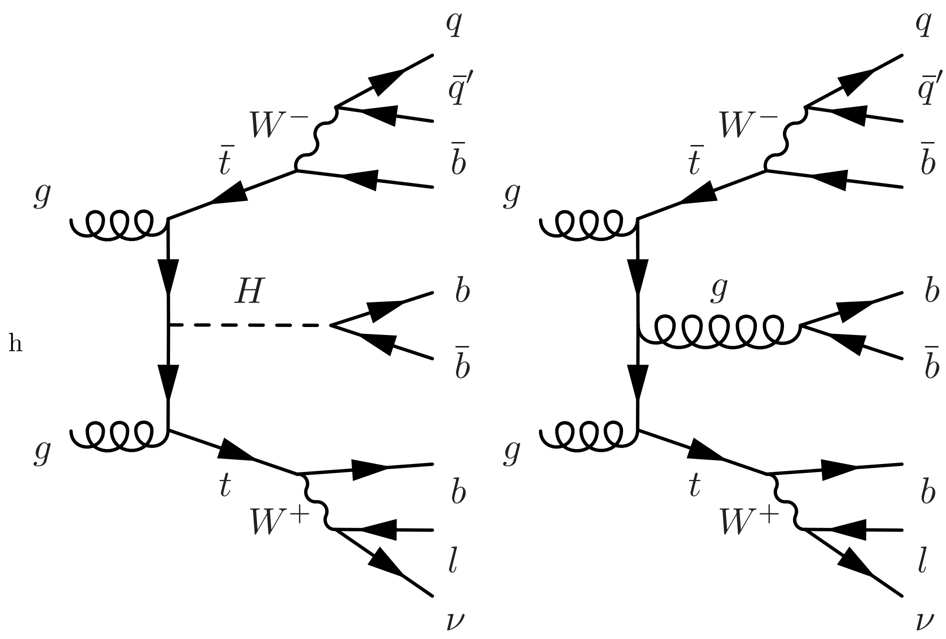

(a) Semileptonic $t\bar{t}H$, with $H \rightarrow\ b\bar{b}$ (b) Semileptonic $t\bar{t} + b\bar{b}$

Figure 2.8: Feynman diagrams for the semileptonic $t\bar{t}H$process and its irreducible background, $t\bar{t} + b\bar{b}$

and $\sqrt{s} = 8\,\text{TeV}$ is given by:

$$\sigma_{ttH} = 0.1293 \quad \pm \quad \text{QCD Scale Unc.}^{+3.8\%}_{-9.3\%} \quad \pm \quad \text{PDF+}\alpha_S \text{ Unc.}^{+8.1\%}_{-8.1\%} \quad \text{pb}^{-1} \tag{2.84}$$

A search for the Higgs in this production mode is additionally challenging due to this large $\sim$ 10% error on the theoretical cross-section. Figure 2.7 shows a Feynman diagram for this process before the branching of the top-quarks or Higgs to final states.

When asking for the Higgs to decay to b-quark pairs, yet another complication arrises when trying to identify which b-quarks came from a top decay or from a Higgs decay. For example, in the semileptonic decay of top quarks, there will be four b-quarks, and two light-flavor quarks in the final state. This means there are 15 (six choose four) possibilities to associate quarks to the top system. Although this is potentially constrained by b-tagging, and kinematic requirements (such as forming the top or W masses), the number of remaining possibilites smears out the resolution on peaking variables such as the invariant mass of b-quark pairs.

2.10 Background Processes to $t\bar{t}H$

The dominant background for $t\bar{t}H$production of top-quark pairs with additional ISR/FSR jets, $t\bar{t} + jets$. The irreducable component of this background is comes when the extra radiation produces a final state with two additional b-quarks, $t\bar{t} + b\bar{b}$. Figure 2.8 compares the Feyman

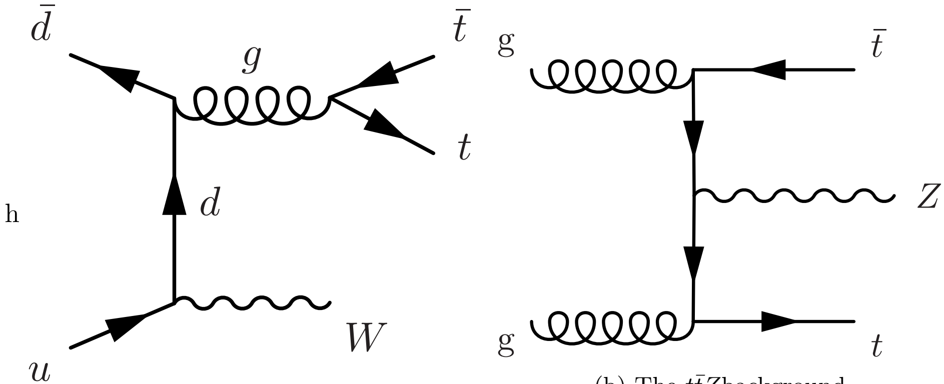

(a) The $t\bar{t}W$background

(b) The $t\bar{t}Z$background

Figure 2.9: Feynman diagrams for the $t\bar{t}W$and $t\bar{t}Z$background processes

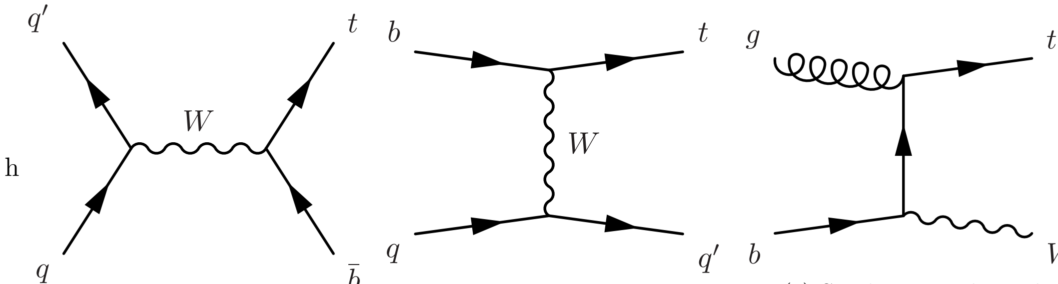

(a) Single t, s-channel

(b) Single t, t-channel

(c) Single t, tW-channel

Figure 2.10: Feynman diagrams for the single t s,t, and tW background processes

diagrams for the semileptonic decays of $t\bar{t}H$and $t\bar{t} + b\bar{b}$.

Additional difficulties come from the theoretical uncertainty on the $t\bar{t} + b\bar{b}$background [28]. The process has been calcualted to NLO QCD in Sherpa [34] and OpenLoops [36] [37] [38]. It has been found that depending on selection cuts, and use of NLO PDF inputs, the difference between LO and NLO calculations on the cross section can be anywhere from 0.99% to 1.96%.

The light flavor component of the $t\bar{t} + jets$background also enters in the selection when any of the jets from the $t\bar{t}$ system or extra radiation are misidentified as b-jets. The cross-section for the $t\bar{t} + jets$process is $\sim 245\,\text{pb}^{-1}$. This is a factor of 1800, so even if a b-tagging algorithm performs with a 1% mis-identification rate of light-jets, there will still be a large contribution from this process that will leave a very similar signature in the detector as $t\bar{t}H$.

The next largest background is the production of vector bosons in association with top-quark pairs, $t\bar{t}W$and $t\bar{t}Z$. Figure 2.9 shows Feynman diagrams from these two processes. They have cross-sections of $\sigma_{ttW} = 0.249\,\text{pb}^{-1}$ and $\sigma_{ttZ} = 0.208\,\text{pb}^{-1}$, which are only a factor of $\sim$2 greater than the $t\bar{t}H$process. These processes can enter the semileptonic $t\bar{t}H$selection by a semileptonic $t\bar{t}$decay, while the vector bosons decay to quarks, or through a hadronic $t\bar{t}$decay, while the vector bosons decay to quarks, and in the case of $t\bar{t}Z$, of the leptons is not identified in the reconstruction.

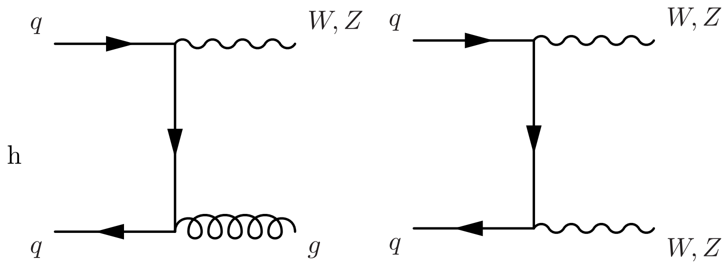

(a) W, Z plus jets (b) DiBoson Production

Figure 2.11: Feynman diagrams for the W, Z plus jets, and diBoson (WW, WZ, ZZ) production.

Single top production is also an important background to consider in a search for $t\bar{t}H$production. Figure 2.10 shows Feynman diagrams for this process. It does not have as large of a contribution as the other backgrounds, since it requires addional radiation in order to have a similar final state jet multiplicity as $t\bar{t}H$. However, since a top-quark is still involved in the process, the final state kinematics of its decay products will be very similar. Single t production has a cross section of $\sigma_t = 71.3\,\mathrm{pb}^{-1}$, while Single $\bar{t}$ production has a cross section of $\sigma_{\bar{t}} = 43.6\,\mathrm{pb}^{-1}$, due to charge asymmetry of the valence quarks of the proton

The last backgorunds to consider are the electroweak production of W and Z bosons in association with jets, as well as WW, WZ, and ZZ pairs in association with jets. Figure **??** shows the Feynman diagrams for these processes, where the V, stands in for wither W or Z bosons. For a semileptonic selection of $t\bar{t}H$events, Z plus jets events enter from a misidentification of one of the leptons from the Z boson decay. Extra FSR/ISR radiation is also to leave a similar signature in the signal region of a $t\bar{t}H$search, so it mainly contributes to control regions of the data.

2.11 Potential BSM Effects on $t\bar{t}H$ production

The phenomological motivation for the existence of physics beyond the Standard Model come from the observation of phenomenon or states of matter not described by the theory. Observations of the cosmic miscrowave background from the Plank telescope have estimated that only $\sim 5\%$ of the observable universe is composed of ordinary matter [39]. The remaining composition is divided between Dark Matter ($\sim 27\%$, and $\sim 68\%$ respecitvely). Evidence for Dark Matter also comes from discrepencies between the observed rotational velocities of galaxies, and the observed mass distributions, suggesting the presence of additional form of matter which does not interact electromagnetically [40].

Additionally, in 1998, the Super-Kamiokande experiment proved that neutrinos oscillated between flavors, implying indirectly that they also have mass [41]. This is something not described in the Standard Model of physics. Due to their neutral charge, these particles are extremely difficult to detect, so experiments have only been able to measure differences in the mass squared between the three mass eigenstates. In 2005, the KamLAND experiment reported $|\Delta m^2_{12} = 0.000079eV^2|$ [42]. In 2006, the MINOS experiment reported $|\Delta m_{23} = 0.0027eV^2|$ [43].

One of the largest theoretical problems with the Standard Model, comes the mechanism which made it all possible- the Higgs. In equation 2.73 there are terms that couple the Higgs boson to itself, $-\lambda v h^3$, and $-\frac{1}{4}\lambda h^4$. When computing NLO effects, these terms lead to a divergence in the Higgs mass, when considering the effect of a loop of fermions on the Higgs propagator. The correctios are of the form $\Delta m_H = -\frac{\lambda_f^2}{8\pi^2}\Lambda_{UV}$. Where Λ_{UV} is the high energy cut off for the theory, which in the limit of a perfect theory, should extend to infinity. This is known as the hierarchy problem.

Beyond the Standard Model physics is a term that describes extensions of the Standard Model in order to describe the observed phenomenon. For the neutrino oscilations, a solution similar to CKM matrix has been proposed, the PontecorvoMakiNakagawaSakata (PMNS) matrix. This proposes that the mass eigenstates of the neutrino are linear combinations of the weak eigenstates, allowing for the mixing of flavors. Current experiments now seek to measure the free parameters of this matrix.

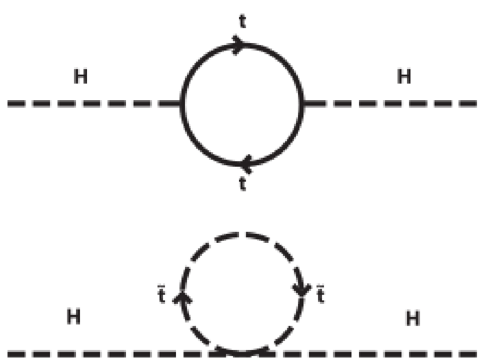

Figure 2.12: The cancellation of the divergent Higgs mass from a loop of top-quarks is cancelled by a loop of supersymmetric top-quarks, stop-quarks,

Both the dark matter and hierarchy problems suffer in the fact that there is no clear model, such as the PMNS matrix, to provide a theoretical solution. Out of the plethora of theories that attempt to solve these problems, supersymmetry (SUSY) is the most popular in the theoretical and experimental community. It suggests that there is a broken symmetry between fermions and bosons, and introduces a partner to each Standard Model particle with a spin quantum number less 1/2 [44]. For the hierarch problem, this provides a set of particles to cancel out the divergences in the NLO corrections to the Higgs mass. Figure 2.12 shows the Feynmann diagrams for a supersymmetric top-quark, or stop quark, that would cancel the divergent contribution from the Standard Model top quark. Depending on the specific form of the SUSY model, the stop quarks can potentially couple directly or indirectly to the top-quark, producing them at a higer rate during pp collisions. This would effect the number of observed events making it into the $t\bar{t}H$ selection.

A number of extensions to the SM also involve introducing new top-like particles into the theory. Vector-like quarks would be spin $1/2$ particles that transform as triplets under the $SU(3)$ color group and whose left and right-handed components have the same color and electroweak quantum numbers [45]. These objects are common to several different types of models. Little Higgs models [46] [47] [48], models with extra dimensions [49] [**?**], top-color models [**?**], and composite Higgs models [**?**], include a vector-like top partner,t' that decays to a top-quark and either a Higgs, W, or Z particle. Both $t't'$ pair production and $t't$ production would yield the ttH final state, or at least one indistinguishable detector signature. $t\bar{t}H$search can provide indirect limits on these models, by observing an excess or lack thereof of $t\bar{t}H$events, without having to directly construct a t' resonance.

Chapter 3

The Large Hadron Collider

The Large Hadron Collider (LHC), is a proton-proton collider operated by the European Center for Nuclear Research (CERN)

3.1 From a bottle of Hydrogen

Our journey begins with a bottle of Hydrogen that is Attached somewhere before being ionized and zipped up to the speed of light.

Such humble beginnings for a tool that is to become the most powerful probe of nature mankind has ever wielded.

3.2 Klystron

This is basically a giant microwave cavity that initially accelerates the protons up to some speed.

3.3 Something Comes Next

Should really know more about how protons get up to these speeds.

3.4 The Main Injector

Then the protons come here and are injected into the LHC

3.5 The LHC Ring

Big magnets, one blew up once, cryogens, vaccuum better than space. Cool.

3.6 Final Structure and Beam Spacing

Bunch structure, talk about important parameters of the beam

Chapter 4

The Compact Muon Solenoid

The Compact Muon Solenoid (CMS) is one of two general purpose detectors at the LHC.

4.1 The Inner Tracker

The inner tracker is silicon and really really big, lots of channels.

4.2 The Electromagnetic Caliorimeter

PBWO4 crystals. APDs in the Barrel. VPTs in the Endcaps

4.2.1 Vacuum Photo-Triodes

Extra time for VPTs

4.2.2 Test Rig at UVa

Big maget, lots of light, test dem led's

4.2.3 Results of UVa Tests

Plots, Plots, plots, plots, plots

4.3 The Hadronic Caliorimeter

Brass, Steel, Soviet Sweat

4.4 Forward Caliorimetry

High eta, great for VBF

4.5 Magnet and Return Yoke

Describe solenoid and measuring field, and engineering marvel or return yoke structure.

4.6 Muon Chambers

APDs DTs and CSCs

4.7 Data Collection Overview

L1 trigger, HLT etc

Chapter 5

Particle Reconstruction at CMS

Data is reconstructed at CMS using the $ParticleFlow^{TM}$ algorithm

5.1 Muon Reconstruction

Muons rely heavily on the inner tracker and muons chambers for efficient identrification and reconstruction

5.2 Electron Reconstruction

Electrons leave charged tracks in the inner tracker, and create a wide shower of particles and thus energy deposits in the ECAL. High energy electrons sometimes traverse the entire distance of the ECAL and leave energy in the HCAL, however the ratio of these two energies is disproportionate for the ECAL, and thus this ratio is often used to discriminate electrons from highly electromagnetic hadronic jets.

5.3 Photon Reconstruction

Like electrons, but with no tracks, and narrower shower shape.

5.4 Jet Reconstruction

Jets are formed by matching tracks from the inner tracker to energy deposits in the ECAL and HCAL. Energy clusters are identified from the ECAL and HCAL, and everything is then clustered in a cone.

5.5 Tau Reconstruction

So heavy that they decay to leptons or hadrons before traversing the detector, they still leave an oddly-numbered pronged decay hadronically due to charge conservation requiring that one of the hadrons produced be eqaul charge to the tau. This results in one charged, and any number of neutral pions, or three charged, and any number of neutral pions.

5.6 Missing Transverse Energy Reconstruction

since the detector is hermetic, and the tracker so granular, we can ensure that no particles flew out of the detector due to lack of coverage. Only long-lived neutral particles can escape, such as neutrinos in the standard model. Many BSM theories, such as SUSY, are characterized by stable, neutral particles.

MET is the vector sum of all of the tracks associated with a particular primary vertex (? or all vertices in event). Thus if there wasa neutral particle that escaped detection, there would be a momentum imbalance along the trajectory of that particle. This is how neutrinos are identified.

Bibliography

[1] CMS Collaboration, "Observation of a new boson at a mass of 125 GeV with the CMS experiment at the LHC", *Phys.Lett.B* (2012) `arXiv:1207.7235`.

[2] ATLAS Collaboration, "Observation of a new particle in the search for the Standard Model Higgs boson with the ATLAS detector at the LHC", *Phys.Lett.B* (2012) `arXiv:1207.7214`.

[3] M. E. Peskin and D. V. Schroeder, "An Introduction to Quantum Field Theory". Westview Press, URL `http://www.westviewpress.com`, 1995.

[4] K. G. Wilson, "Renormalization Group and Critical Phenomena. I. Renormalization Group and the Kadanoff Scaling Picture", *Phys. Rev. B* **4** (Nov, 1971) 3174–3183, `doi:10.1103/PhysRevB.4.3174`.

[5] K. G. Wilson, "Renormalization Group and Critical Phenomena. II. Phase-Space Cell Analysis of Critical Behavior", *Phys. Rev. B* **4** (Nov, 1971) 3184–3205, `doi:10.1103/PhysRevB.4.3184`.

[6] S. Bethke, "The 2009 World Average of alpha(s)", *Eur.Phys.J.* **C64** (2009) 689–703, `doi:10.1140/epjc/s10052-009-1173-1`, `arXiv:0908.1135`.

[7] H. Weyl, "The theory of groups and quantum mechanics". Dover Press, URL `https://ia700807.us.archive.org/20/items/ost-chemistry-quantumtheoryofa029235mbp/quantumtheoryofa029235mbp.pdf`, 1930.

[8] C. N. Yang and R. L. Mills, "Conservation of Isotopic Spin and Isotopic Gauge Invariance", *Phys. Rev.* **96** (Oct, 1954) 191–195, `doi:10.1103/PhysRev.96.191`.

[9] M. Gell-Mann, "A Schematic Model of Baryons and Mesons", *Phys.Lett.* **8** (1964) 214–215, `doi:10.1016/S0031-9163(64)92001-3`.

[10] G. Zweig, "An SU_3 model for strong interaction symmetry and its breaking; Version 1", Technical Report CERN-TH-401, CERN, Geneva, Jan, 1964.

[11] G. Zweig, "An SU_3 model for strong interaction symmetry and its breaking; Version 2",.

[12] O. W. Greenberg, "Spin and Unitary-Spin Independence in a Paraquark Model of Baryons and Mesons", *Phys. Rev. Lett.* **13** (Nov, 1964) 598–602, `doi:10.1103/PhysRevLett.13.598`.

[13] P. Higgs, "Broken symmetries, massless particles and gauge fields", *Physics Letters* **12** (1964), no. 2, 132 – 133, `doi:http://dx.doi.org/10.1016/0031-9163(64)91136-9`.

[14] S. Weinberg, "A Model of Leptons", *Phys. Rev. Lett.* **19** (Nov, 1967) 1264–1266, `doi:10.1103/PhysRevLett.19.1264`.

[15] S. L. Glashow, "Partial-symmetries of weak interactions", *Nuclear Physics* **22** (1961), no. 4, 579 – 588, `doi:http://dx.doi.org/10.1016/0029-5582(61)90469-2`.

[16] A. Salam and J. Ward, "Electromagnetic and weak interactions", *Physics Letters* **13** (1964), no. 2, 168 – 171, `doi:http://dx.doi.org/10.1016/0031-9163(64)90711-5`.

[17] Nobelprize.org, "The Nobel Prize in Physics 1957". URL `http://www.nobelprize.org/nobel_prizes/physics/laureates/1957/`.

[18] N. Cabibbo, "Unitary Symmetry and Leptonic Decays", *Phys. Rev. Lett.* **10** (Jun, 1963) 531–533, `doi:10.1103/PhysRevLett.10.531`.

[19] M. Kobayashi and T. Maskawa, "CP Violation in the Renormalizable Theory of Weak Interaction", *Prog.Theor.Phys.* **49** (1973) 652–657, `doi:10.1143/PTP.49.652`.

[20] G. Arnison et al., "Experimental observation of isolated large transverse energy electrons with associated missing energy at s=540 GeV", *Physics Letters B* **122** (1983), no. 1, 103 – 116, `doi:http://dx.doi.org/10.1016/0370-2693(83)91177-2`.

[21] G. Arnison et al., "Experimental observation of lepton pairs of invariant mass around 95 GeV/c2 at the {CERN} {SPS} collider", *Physics Letters B* **126** (1983), no. 5, 398 – 410, `doi:http://dx.doi.org/10.1016/0370-2693(83)90188-0`.

[22] M. Banner et al., "Observation of single isolated electrons of high transverse momentum in events with missing transverse energy at the {CERN} pp collider", *Physics Letters B* **122** (1983), no. 56, 476 – 485, `doi:http://dx.doi.org/10.1016/0370-2693(83)91605-2`.

[23] P. Bagnaia et al., "Evidence for Z0e+e at the {CERN} pp collider", *Physics Letters B* **129** (1983), no. 12, 130 – 140, `doi:http://dx.doi.org/10.1016/0370-2693(83)90744-X`.

[24] The ALEPH, DELPHI, L3, OPAL, SLD Collaborations, the LEP Electroweak Working Group, the SLD Electroweak and Heavy Flavour Groups, "Precision Electroweak Measurements on the Z Resonance", *Phys. Rept.* **427** (2006) 257, `arXiv:hep-ex/0509008`.

[25] The ALEPH, DELPHI, L3, OPAL Collaborations, the LEP Electroweak Working Group, "Electroweak Measurements in Electron-Positron Collisions at W-Boson-Pair Energies at LEP", *Phys. Rept.* **532** (2013) 119, `arXiv:1302.3415`.

[26] F. Abe et al., "Observation of Top Quark Production in $\overline{p}p$ Collisions with the Collider Detector at Fermilab", *Phys. Rev. Lett.* **74** (Apr, 1995) 2626–2631, `doi:10.1103/PhysRevLett.74.2626`.

[27] S. Abachi et al., "Search for High Mass Top Quark Production in $p\overline{p}$ Collisions at $\sqrt{s} =$ 1.8 TeV", *Phys. Rev. Lett.* **74** (Mar, 1995) 2422–2426, `doi:10.1103/PhysRevLett.74.2422`.

[28] LHC Higgs Cross Section Working Group Collaboration, "Handbook of LHC Higgs Cross Sections: 3. Higgs Properties", `doi:10.5170/CERN-2013-004`, `arXiv:1307.1347`.

[29] W. Beenakker et al., "Higgs radiation off top quarks at the Tevatron and the LHC", *Phys.Rev.Lett.* **87** (2001) 201805, `doi:10.1103/PhysRevLett.87.201805`, `arXiv:hep-ph/0107081`.

[30] W. Beenakker et al., "NLO QCD corrections to t anti-t H production in hadron collisions", *Nucl.Phys.* **B653** (2003) 151–203, `doi:10.1016/S0550-3213(03)00044-0`, `arXiv:hep-ph/0211352`.

[31] R. Frederix et al., "Scalar and pseudoscalar Higgs production in association with a top-antitop pair", *Phys.Lett.* **B701** (2011) 427–433, `doi:10.1016/j.physletb.2011.06.012`, `arXiv:1104.5613`.

[32] M. Garzelli, A. Kardos, C. Papadopoulos, and Z. Trocsanyi, "Standard Model Higgs boson production in association with a top anti-top pair at NLO with parton showering", *Europhys.Lett.* **96** (2011) 11001, `doi:10.1209/0295-5075/96/11001`, `arXiv:1108.0387`.

[33] S. Dawson, L. Orr, L. Reina, and D. Wackeroth, "Associated top quark Higgs boson production at the LHC", *Phys.Rev.* **D67** (2003) 071503, `doi:10.1103/PhysRevD.67.071503`, `arXiv:hep-ph/0211438`.

[34] T. Gleisberg et al., "Event generation with SHERPA 1.1", *JHEP* **0902** (2009) 007, `doi:10.1088/1126-6708/2009/02/007`, `arXiv:0811.4622`.

[35] P. Artoisenet, R. Frederix, O. Mattelaer, and R. Rietkerk, “Automatic spin-entangled decays of heavy resonances in Monte Carlo simulations”, *JHEP* **1303** (2013) 015, `doi:10.1007/JHEP03(2013)015`, `arXiv:1212.3460`.

[36] F. Cascioli, P. Maierhofer, and S. Pozzorini, “Scattering Amplitudes with Open Loops”, *Phys.Rev.Lett.* **108** (2012) 111601, `doi:10.1103/PhysRevLett.108.111601`, `arXiv:1111.5206`.

[37] F. Krauss, R. Kuhn, and G. Soff, “AMEGIC++ 1.0: A Matrix element generator in C++”, *JHEP* **0202** (2002) 044, `doi:10.1088/1126-6708/2002/02/044`, `arXiv:hep-ph/0109036`.

[38] T. Gleisberg and F. Krauss, “Automating dipole subtraction for QCD NLO calculations”, *Eur.Phys.J.* **C53** (2008) 501–523, `doi:10.1140/epjc/s10052-007-0495-0`, `arXiv:0709.2881`.

[39] Planck Collaboration, “Planck 2013 results. I. Overview of products and scientific results”, *Astron.Astrophys.* **571** (2014) A1, `doi:10.1051/0004-6361/201321529`, `arXiv:1303.5062`.

[40] V. Rubin, N. Thonnard, and J. Ford, W.K., “Rotational properties of 21 SC galaxies with a large range of luminosities and radii, from NGC 4605 /R = 4kpc/ to UGC 2885 /R = 122 kpc/”, *Astrophys.J.* **238** (1980) 471, `doi:10.1086/158003`.

[41] Super-Kamiokande Collaboration Collaboration, “Measurements of the solar neutrino flux from Super-Kamiokande’s first 300 days”, *Phys.Rev.Lett.* **81** (1998) 1158–1162, `doi:10.1103/PhysRevLett.81.1158`, `arXiv:hep-ex/9805021`.

[42] KamLAND Collaboration Collaboration, “Measurement of neutrino oscillation with KamLAND: Evidence of spectral distortion”, *Phys.Rev.Lett.* **94** (2005) 081801, `doi:10.1103/PhysRevLett.94.081801`, `arXiv:hep-ex/0406035`.

[43] MINOS Collaboration Collaboration, “Observation of muon neutrino disappearance with the MINOS detectors and the NuMI neutrino beam”, *Phys.Rev.Lett.* **97** (2006) 191801, `doi:10.1103/PhysRevLett.97.191801`, `arXiv:hep-ex/0607088`.

[44] S. P. Martin, “A Supersymmetry primer”, *Adv.Ser.Direct.High Energy Phys.* **21** (2010) 1–153, `doi:10.1142/9789814307505_0001`, `arXiv:hep-ph/9709356`.

[45] J. Aguilar-Saavedra, R. Benbrik, S. Heinemeyer, and M. Prez-Victoria, “Handbook of vectorlike quarks: Mixing and single production”, *Phys.Rev.* **D88** (2013), no. 9, 094010, `doi:10.1103/PhysRevD.88.094010`, `arXiv:1306.0572`.

[46] G. Burdman, M. Perelstein, and A. Pierce, "Large Hadron Collider tests of a little Higgs model", *Phys.Rev.Lett.* **90** (2003) 241802, `doi:10.1103/PhysRevLett.90.241802`, `arXiv:hep-ph/0212228`.

[47] M. Perelstein, M. E. Peskin, and A. Pierce, "Top quarks and electroweak symmetry breaking in little Higgs models", *Phys.Rev.* **D69** (2004) 075002, `doi:10.1103/PhysRevD.69.075002`, `arXiv:hep-ph/0310039`.

[48] H.-C. Cheng, I. Low, and L.-T. Wang, "Top partners in little Higgs theories with T parity", *Phys. Rev. D* **74** (Sep, 2006) 055001, `doi:10.1103/PhysRevD.74.055001`.

[49] H.-C. Cheng, B. A. Dobrescu, and C. T. Hill, "Electroweak symmetry breaking and extra dimensions", *Nucl.Phys.* **B589** (2000) 249–268, `doi:10.1016/S0550-3213(00)00401-6`, `arXiv:hep-ph/9912343`.

List of Acryonyms

ATLAS A Toroidal LHC Apparatus

BSM Beyond the Standard Model

CERN European Center for Nuclear Research

CMS Compact Muon Solenoid

FSR Final State Radiation

ISR Initial State Radiation

JHEP Journal of High Energy Physics

LHC Large Hadron Collider

LO Leading Order

MVA Multi-Variate Analysis

NLO Next to Leading Order

QCD Quantum Chromodynamics

QED Quantum Electrodynamics

QFT Quantum Field Theory

SM Standard Model